University of Twente

Compensation of Friction in the Flight Simulator Stick using an Adaptive Friction Compensator

Nathan van Seters

M.Sc. Thesis

Author:	N. van Seters	Control Laboratory Faculty of Electrical Engineering
Supervisors:	Prof. dr. ir. J. van Amerongen Dr. ir. T.J.A. de Vries Dr. ir. J. van Dijk Ir. E. Schrijver	University of Twente P.O. Box 217 7500 AE Enschede The Netherlands

Date:	06/19/01	Reportnumber: 006R2001

Abstract

Friction deteriorates the performance of many controlled systems with moving parts. It introduces not wanted phenomena to the system, such as stick-slip, steady state errors and tracking errors nearby velocity reversals (the so-called reversal bumps). However, it is possible to compensate for the friction in order to reduce the not wanted friction phenomena. In previous research at the Control Laboratory the friction, in particular the reversal bump, has been compensated for with learning friction compensators. These compensators were able to reduce the reversal bump significantly. Besides learning friction compensation there are other compensation techniques. One of them is adaptive friction compensation. The use of adaptive friction compensation seems well suited because it is known that friction will vary in time, due to wear and temperature changes. An adaptive friction compensator is capable of following these variations in friction.

In this thesis three adaptive friction compensators are presented. One is based on the Coulomb friction model and two of them are based on the LuGre friction model. In simulations the adaptive Coulomb friction compensator was able to reduce the reversal bump by a factor 6. The LuGre based adaptive compensators where able to eliminate the reversal bump in simulations, this mainly caused by the fact that the 'real' friction was also represented by the LuGre model.

In order to verify the results of the simulations, the adaptive friction compensators are implemented on the control loading system (flight simulator stick) of FCS. This system is available at the Control Laboratory and also used to implemented the learning friction compensators, so the performances of both techniques could be compared easily. First the friction on the control loading system has been identified (i.e. the LuGre model parameters), for both the simulations and the initial values of the compensators. The three adaptive compensators have been implemented on the Control Loading System. The Coulomb based compensator was also in experiments able to reduce the reversal bump, by a factor 7. The first LuGre based compensator was also able to reduce the reversal bump, however due to computation difficulties this was not what was hoped for. The last adaptive compensator was not capable of reducing the reversal bump at all.

When both friction compensation techniques, learning and adaptive, are compared to each other one could say that both techniques are able to reduce the reversal bump. Even the simplest adaptive compensator, the Coulomb friction compensator, is not inferior to the learning friction compensators. And this compensator is easy to implement on a system and requires no a-priori knowledge (which is the main advantage of learning compensation).

Preface

After six years of study at the University of Twente, I finally reach the end of the time of being a student. It have been a great time, wherein study and leisuretime rapidly alternated.

The past one and a half year I have been working at the Control Laboratory. Due to several causes this has been longer than planned. However these 'problems' have been overcome and the end is here. I would like to thank Theo de Vries for giving me this assignment and giving me critical notes concerning this thesis and during this assignment. I want to thank everyone at the Control Laboratory for their support whenever asked for. Especially the students who are working for their M. Sc. assignment for their support when there was a problem and the many discussions during lunchtime. It was pleasant to work with you.

A special thanks goes to mine parents and sister Ilja for their mental support whenever needed and their faith in me all these years. Beside the mental support I would like to thank them for their financial support.

Futhermore I want to thank the inmates at the Padangstraat for the lots of fun, 'Quaken' and 'paaltjesvoetbal' in the 'garden'. It has been a great stress reliever after hours of studying and hard working. The same applies to mine friends at the Stretchers. I thank them for the many hours of sportpleasure and the many evenings of playing 'Siedler'. Finally I would like to thank the friends at the faculty of Electrical Engineering for the time of studying together, tackling problems and the many projects done together.

Nathan van Seters
Enschede, Juni 2001

Contents

1 Introduction

Friction is a phenomenon that is present during the relative motion of two surfaces in contact. Sometimes the presence of friction is welcome, for example in braking systems or with the motion of wheels (by cars and bicycles), but friction is generally a limition of the performance of controlled electromechanical motion systems. To increase the performance of such systems, it is necessary to compensate for the friction. In literature, several techniques are suggested for friction compensation. One of these techniques, adaptive compensation, will be studied in this thesis.

1.1 Background

Friction occurs in all mechanical systems and it appears at the physical interface between two surfaces in contact. Friction serves to provide damping at all frequencies. At the upper limits of performance, friction will affect the design of time optimal control and determine the limits of speed and power. However friction posses its greatest challenge at the lower limit of the performance, for small motions and velocities (Armstrong-Hélouvry, B., 1991). The influence of the nonlinearity of friction is the biggest at low velocities and velocity reversals. Phenomena like hunting cycles, steady state errors and stick-slip are generated by the low velocity friction. The friction characteristic shows a discontinuity at zero velocity, see
Figure 1-1. This causes the system to get stuck at velocity reversals resulting in a velocity and acceleration error. This is shown schematically in Figure 1-2.

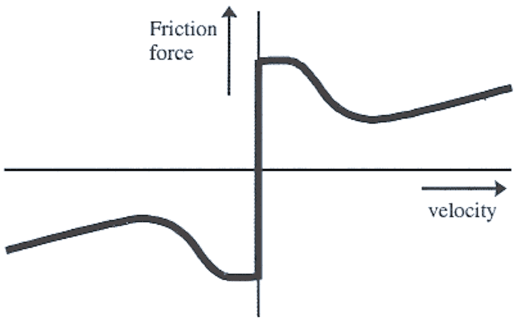

Figure 1-1 Friction force versus the velocity

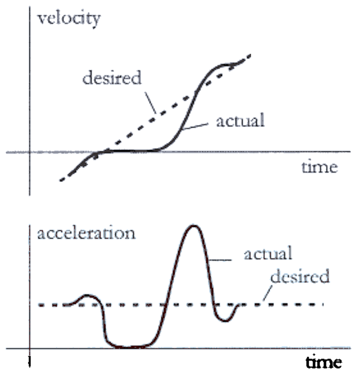

Figure 1-2 The velocity and acceleration at a velocity reversal

This effect at velocity reversals due to the friction is called "reversal bump" and decreases the performance of a motion system.

Friction was studied extensively in classical mechanical engineering and there has lately been a strong resurgence (Olsson, H. et al., 1998). Apart from intellectual curiosity, this is driven by strong engineering needs in a wide range of industries from disc drives to cars.

The availability of new precise measurement techniques has also been a good push forward.

For control engineers it is important to understand friction phenomena and to know how to deal with the effects of it. With the availability of more powerful computers it is in many cases possible to deal with the effects of friction. This has the potential to improve quality, economy and safety of a system (Olsson, H. et al., 1998). When a system or machine is designed, friction should be considered early in the system design stage, by reducing it as much as possible. This can be achieved by a good hardware design and a good choice of lubricant. However, if the desired performances are still not met and the system is mechanically optimal, friction compensation by means of control engineering is necessary.

An example of a system where the friction has great influence on the performance is the control loading system of Fokker Control Systems (FCS). The control loading system (FCLS) present at the Control Laboratory of the University of Twente is depicted in Figure 1-3.

Figure 1-3 The Fokker Control Loading System

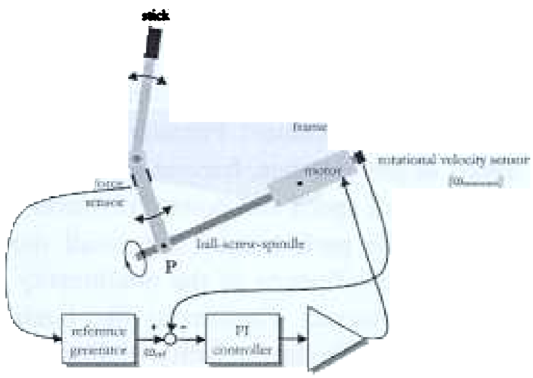

Figure 1-4 Fokker Control Loading System schematically

The system consists of a stick, which is attached via a transmission to a motor, see Figure 1-4. The transmission consists of a ball-screw-spindle which transforms the rotation of the motor into a translation the point P. This in turn will rotate both the stick and the motor. The motor is controlled in a velocity loop with a PI controller. The motor velocity is measured with a tacho-sensor. Besides the motor velocity also the motor position is measured with an encoder. A reference generator calculates the reference rotational velocity from a simulation model (for example an airplane controls model) which has as input the applied force.
Fokker Control Systems uses such systems in their simulators, e.g. flight simulators. With a regular controller without friction compensation, the operator can clearly feel a reversal bump when changing the motion direction of the stick. This is undesirable, because it makes the behavior of the simulator less realistic. Therefore, friction compensation is added to reduce the reversal bump to such a level that the operator can not feel it anymore. In previous research on this subject, a learning friction compensator was developed for the

FCLS (Spreeuwers, L., 1999). With this compensation technique, the reversal bump can be reduced below the level of perception. Nevertheless, there are alternative techniques to reduce the influence of friction. One of these techniques, adaptive compensation, seems well suited. The friction parameters may vary in time, due to temperature changes, wear or variable loads. An adaptive compensator can deal with such variances, whereas the learning compensator cannot (at present).

1.2 Assignment

In order to assess the performance of the learning friction compensator of (Spreeuwers, L., 1999), other compensators need to be designed and implemented. One compensation technique that seems well suited is adaptive friction compensation.
A major effect of friction on the control loading system is the reversal bump. The compensators will be compared with each other by looking at the way in which the compensators deal with the reversal bump.

The assignment can be summarized as:

The design and implementation of an adaptive control system that compensates for friction.

The adaptive friction compensator has to be implemented on the control loading system (flight simulator stick) of Fokker Control Systems. The adaptive compensator has to be tested under the same operating conditions as the learning compensators. This means that the same PI controller has to be used (with the same values for the parameters) and the same reference path in order to compare this compensators fairly.
Before the compensator can be designed and implemented, some insight in friction and its phenomena is needed. The knowledge of friction and its phenomena results in friction models, where the friction phenomena are described.

The assignment can be divided into four parts:

1. Study of the friction phenomena, friction models and friction compensation techniques,
2. Design and simulation of an adaptive friction compensator that compensates friction and reduces the reversal bump,
3. Implementation and test of the adaptive friction compensator on the control loading system of FCS,
4. Comparison of the adaptive and learning friction compensators based on the results of the experiments.

1.3 Thesis outline

In order to get a better understanding of friction and its phenomena an overview of literature related to friction is given in chapter 2. In this chapter the friction phenomena, the friction models and compensation techniques are discussed, resulting in an overview of adaptive friction compensators found in literature and a comparison of adaptive compensation and learning compensation.
Some of the adaptive compensation techniques found in the literature will be discussed in detail, and a design for the FCLS will be presented and simulated in chapter 3.

In chapter 4 the results of the experiments of the adaptive friction compensators on the control loading system of FCS will be given attention. The comparison between adaptive and learning compensators based on the result of the experiments will also be dealt within this chapter.
Finally conclusions will be drawn and recommendations will be given in chapter 5.

Friction

Friction is a phenomenon that is present during the relative motion of surfaces in contact. It is the tangential reaction force between the surfaces in contact. These reaction forces are the result of many different mechanisms, which depend on properties of the bulk and surface materials of the bodies, displacement and relative velocity of the bodies, contact geometry and topology and the presence of lubrication (Olsson, H. et al., 1998).
The presence of friction is sometimes of great importance and welcome, for instance in braking systems or with the motions of wheels. However, friction is generally a limitation of the performance of controlled electromechanical motion systems. These limitations manifest themselves in steady state errors, limit cycles, tracking errors nearby velocity reversals (reversal bumps) and stick-slip. To be able to reduce the (negative) effects of friction it is necessary to have a deeper understanding in friction phenomena and friction models.
The chapter on Friction of (Spreeuwers, L., 1999) is used as a guideline for this chapter. In paragraph 2.1 phenomena of friction will be discussed. In the next paragraph the behavior of friction around zero velocity due to lubrication is treated. The friction models derived from the friction phenomena are dealt with in paragraph 2.3. In paragraph 2.4 several friction compensation techniques are discussed. This paragraph ends with a survey of adaptive friction compensators found in literature. The last paragraph, paragraph 2.5, is devoted to a comparison between adaptive friction compensation and learning friction compensation.

2.1 Friction phenomena

In this section definitions of some commonly used friction phenomena are given:

- *Static friction*
  Static friction is the friction when the two surfaces are sticking. The force required to overcome the static friction and initiate motion is called the breakaway force. The static friction is usually larger than the Coulomb friction.
- *Coulomb friction*
  Coulomb friction is independent of velocity and is always present. This friction component is only dependent on the direction of motion, in such way that it is in the direction opposite to the velocity. The magnitude of Coulomb friction depends on the properties of the surfaces in contact and the normal force. Coulomb friction is also known as kinetic friction or dynamic friction.
- *Viscous friction*
  Viscous friction is dependent of the (magnitude of the) velocity. At zero velocity the viscous friction is zero and the viscous friction component increases with the increase of velocity.
- *Stribeck friction*
  Stribeck friction arises from the usage of fluid lubrication. At low velocity the friction will decrease with the increase of velocity.

Pre-sliding displacement
Pre-sliding displacement is a friction phenomenon that arises from the elastic deformation of bonding sites between two surfaces when the applied force has not exceeded the breakaway force (static friction). The sliding junction behaves as a linear spring for small displacements. Pre-sliding displacement is sometimes referred to as the Dahl effect.
Varying break-away force
Varying breakaway force is the dependency of the breakaway force on the rate of increase of the applied force.
Frictional lag
Frictional lag is the delay in the change of the friction force as a function of a change in the velocity.

In literature other effects regarding to friction are reported besides the above mentioned friction phenomena:

- *Direction dependent friction*
  The friction phenomena mentioned above might be dependent on the direction of the velocity (Armstrong-Hélouvry, B., 1991; Armstrong-Hélouvry, B. et al., 1994; Canudas de Wit, C. et al., 1987; Leonard, N.E. and Krishnaprasad, P.S., 1992). The level of Coulomb and static friction can be different in opposite directions. For example in the control loading system available on the Control Laboratory (and used for the experiments) this effect is present. The cause of this dependency can be anisotropies in the material, geometry or surface conditions.
- *Time dependent friction*
  It is known from experiments that friction changes with time (Armstrong-Hélouvry, B. et al., 1994; Canudas de Wit, C. et al., 1987; Feemster, M. et al., 1999; Leonard, N.E. and Krishnaprasad, P.S., 1992). Possible causes of time dependency of friction may be temperature changes (due to heat generated by the friction itself or by an external source), wear of the surfaces, loss of lubricant or deformation of the surface material other than wear.
- *Position dependent friction*
  Friction, as showed in experiments (Armstrong-Hélouvry, B., 1991; Armstrong-Hélouvry, B. et al., 1994; Canudas de Wit, C. et al., 1987), can be position dependent. This can be caused by an inhomogeneous contact area for the range of motion.

2.2 Four dynamic regimes

Despite the many different lubricants available to decrease the effects of friction, the lubricants can not eliminate the friction totally (Armstrong-Hélouvry, B., 1991). Some friction effects remain in the system or can not be reduced sufficiently. In a system with grease or oil, four regimes of lubrication can be distinguished, each with different phenomena of friction dominant: static friction, boundary lubrication, partial fluid lubrication and full fluid lubrication. These four regimes each contribute to the dynamics that a controller confronts as the system accelerates away from zero velocity. In figure 2-1 the curve, known as the Stribeck curve, is plotted for the three moving regimes.

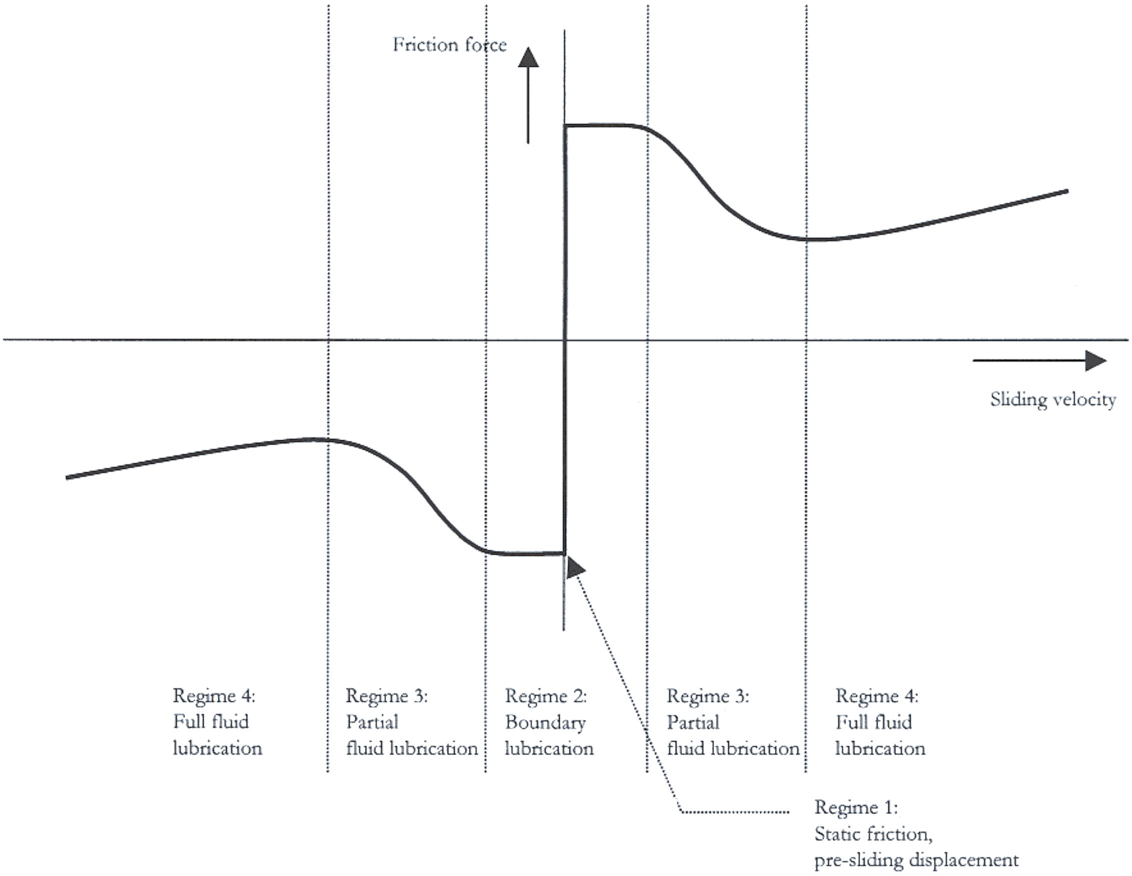

Figure 2-1 The four dynamic regimes of friction (friction force versus sliding velocity)

The characteristics of the static friction are not dependent on velocity. A description of the four regimes is given next (Armstrong-Hélouvry, B., 1991):

- *Regime 1: Static friction*
  In figure 2-2a a contact is shown to occur at asperity junctions. These junctions have two behaviors important in this regime. First both the surface film and the asperities deform plastically under the load, which can lead to increasing static friction as the junction spends more time at zero velocity. Second the junctions deform elastically, so the contact area appears to be a solid connection with a stiff spring. That is, the force is a linear function of the displacement, up to a critical displacement or force at which breakaway occurs. The transition from pre-sliding displacement to sliding is not abrupt: the sliding starts at the boundary of a contact and then it propagates toward the center.
- *Regime 2: Boundary lubrication*
  In this regime the velocity is not adequate to build a fluid film between the surfaces, see figure 2-2b. The boundary layer of the surfaces serves to provide lubrication. The friction in the boundary lubrication regime is, in most cases, higher than the regimes with fluid lubrication (the next regimes).
- *Regime 3: Partial Fluid Lubrication*
  In this regime the lubricant is brought into the load bearing region through motion, either by sliding or rolling. The pressure arising from the load will expel some of the lubricant, but viscosity prevents all of the lubricant from escaping and a film is formed, see figure 2-2c. This process is dominated by the interaction of lubricant viscosity, the velocity and contact geometry. The greater the viscosity or velocity, the thicker the fluid film will be. When the film is not thicker than the height of the asperities, some solid-to-solid contact will remain. These contacts will decrease with

the increase of the velocity, resulting in less friction (fluid lubrication will in most cases reduce friction in regard to solid-to-solid friction). This is called the Stribeck effect.

Regime 4: Full Fluid Lubrication

All solid-to-solid contacts are eliminated in this regime, see figure 2-2d. The dominant friction phenomenon, besides the always present Coulomb friction, is viscous friction. The wear in this regime is reduced by orders of magnitude.

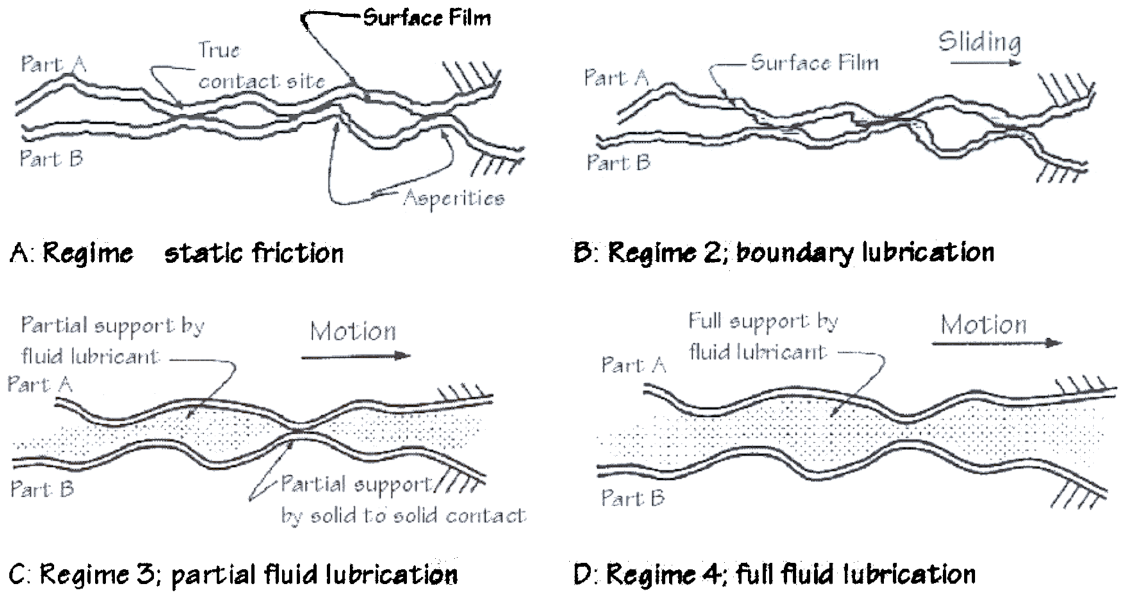

Figure 2-2 Four dynamic regimes visualized

2.3 Friction models

In order to simulate and design a controller (with or without friction compensation) it is necessary to use a model for friction. The accuracy of the simulations and which effect is taken into account determine which model can be used. Each friction model incorporates one or more friction phenomena. The friction phenomena can be grouped into static and dynamic friction phenomena:

- Static friction phenomena
  - Static friction
  - Coulomb friction
  - Viscous friction
  - Stribeck friction
- Dynamic friction phenomena
  - Pre-sliding displacement
  - Rising static friction
  - Frictional lag

Together with the phenomena the models can be divided into two groups, static models and dynamic models. Static friction models incorporate only static friction phenomena and are a static function of velocity. Dynamic friction models contains besides static friction phenomena also some dynamic friction phenomena (Altpeter, F. et al., 1997).

Other effects like time-dependent friction and position-dependent friction are more difficult to catch in a model. Time dependency of friction is unpredictable and position dependency is difficult to include in a model. Direction dependency is subject to the system, but it is easier to include in a model.

2.3.1 Static friction models

The static friction models have a static dependency on velocity. The first friction model goes back to Leonardo da Vinci. Da Vinci stated that friction is proportional to the load, opposed to the direction of the motion and independent of the contact area. Coulomb (1785) developed this model further, and the result became known as Coulomb friction. The model is given in figure 2-3.

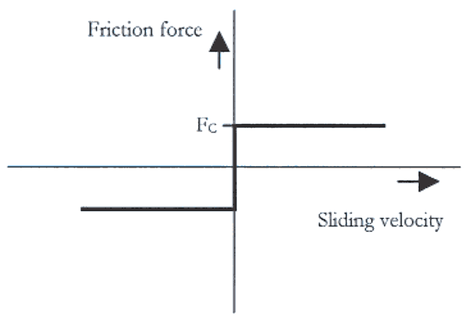

Figure 2-3 The Coulomb friction model

Morin introduced in 1833 the idea of static friction into the friction models. Reynolds (1866) developed expressions for the friction force caused by the viscosity of lubricants, which is referred to as viscous friction. The combination of Coulomb, static and viscous friction is most commonly used in engineering (Armstrong-Hélouvry, B., 1991). The model is given in figure 2-4.

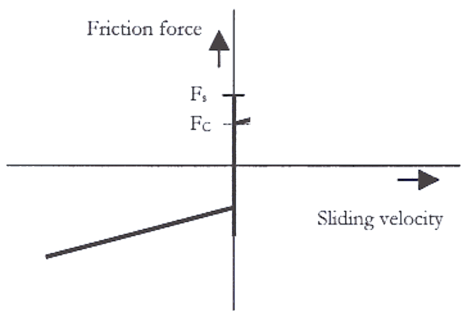

Figure 2-4 The Coulomb plus static plus viscous friction model

In 1902 Stribeck formulated a new model where he included his observation that for low velocities the friction force normally decreases continuously with increasing velocity and not in a discontinuous way, as is the case in the Coulomb plus static plus viscous friction model. In figure 2-5 the model including Coulomb, viscous and Stribeck friction is given. There are several formulas for the Stribeck friction available.

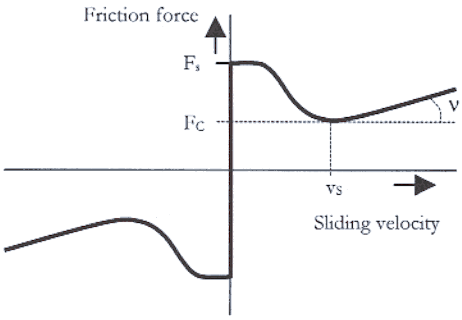

Figure 2-5 The Coulomb plus viscous plus Stribeck friction model

At the Control Laboratory a new static friction model has been developed (Breedveld, P.C., 2000). The model incorporates static friction, Coulomb friction and rising static friction and is made using a port-based approach. The model is made so that it is re-usable and numerically robust and efficient for simulations (Breedveld, P.C., 2000).

A major problem of the static friction models during simulation is the discontinuity at zero velocity. At zero velocity the friction force is not a function of the velocity, but a function of the applied force. The friction force has the same magnitude as the applied force, but in the opposite direction. So the effective force is zero. When the applied force excees the level of Coulomb or static friction (depends on the choice of the model) the friction force becomes either the Coulomb friction level or the static friction level.
The detection of the zero velocity discontinuity in simulations with the static friction models make the simulations less efficient (Armstrong-Hélouvry, B. et al., 1994). There are some measures that can be taken to reduce this problem, like a small band around zero to overcome the detection of zero or replacing the discontinuity by a continuous function (arctan) or a (*piece-wise*) linear function through zero (Breedveld, P.C., 2000).

2.3.2 Dynamic friction models

In addition to static friction models, there are dynamic friction models. The dynamic friction models include besides the static friction components also some dynamic aspects of friction. Dynamic friction models have been developed from different approaches.

One model that incorporate all mentioned friction phenomena (paragraph 2.1) is the *seven parameter model of Armstrong* (Armstrong-Hélouvry, B., 1991; Armstrong-Hélouvry, B. et al., 1994). This model is obtained by modifying a static friction model and exists of two separate equations for sliding and sticking. The equation to describe sticking is an equation of a spring and incorporate pre-sliding displacement. The sliding equation describes besides the static friction phenomena, frictional lag and rising static friction. A mechanism has to supervise the switching between the model for sticking and the model for sliding. After every switch, the model states have to be initialized properly.

The next class of dynamic friction models are developed using another approach to friction. These models are simplified representations of the physical contacts between surfaces where friction takes place. In this way the models incorporate the dynamic phenomena more naturally (Spreeuwers, L., 1999). Examples of such models are the Dahl model, the Bliman-Sorine model and the LuGre model. The LuGre model will be explained more extensively, because this is one of the models used for friction compensation.

The *Dahl model* is based on two considerations (Spreeuwers, L., 1999):
1. The origin of friction is in quasi-static "bonds" that are continuously formed and subsequently broken.
2. The resulting functions behave as a brush whose bristles must be bent as the brush moves in one direction and then flop or bend in the opposite direction if the motion is reversed.

The Dahl model contains only Coulomb friction of the static friction phenomena and pre-sliding displacement of the dynamic friction phenomena.

In order to incorporate the Stribeck effect in the dynamic friction model, Bliman and Sorine extended the Dahl model. The Bliman-Sorine model is a second order model and can be viewed as a parallel connection of two Dahl models (Canudas de Wit, C. et al., 1995; Gäfvert, M., 1996). The Bliman-Sorine model contains static, viscous and Coulomb friction of the static friction phenomena and pre-sliding displacement of the dynamic friction phenomena (Gäfvert, M., 1996).

The LuGre friction model can also been seen as an extension of the Dahl model. The LuGre model will now be discussed more extensively.

LuGre friction model

The LuGre model was introduced in 1995 (Canudas de Wit, C. et al., 1995). The model is inspired by the bristle interpretation of friction. The contact area of two surfaces is visualized as two rigid bodies that make contact through elastic bristles. These bristles will deflect like springs when a tangential force is applied. With the deflection of the bristles the friction force will rise.

If the force is sufficiently large some of the bristles deflect so much that they will slip. This phenomenon is highly random due to the irregular forms of the surface. In (Canudas de Wit, C. et al., 1995) a model is proposed that is based on the average behavior of the bristles. The average deflection (z) is modeled by

$$\frac{dz}{dt} = \dot{x} - \frac{|\dot{x}|}{g(\dot{x})} z$$

with v the relative velocity between the two surfaces.

The function $g(\dot{x})$ is positive and depend on many factors such as material properties, lubrication and temperature. In (Canudas de Wit, C. et al., 1995) the following function for $g(\dot{x})$ is proposed which captures the Stribeck effect

$$\sigma_0 g(\dot{x}) = F_C + (F_S - F_C)e^{-\left(\frac{\dot{x}}{v_s}\right)^2}$$

where F_C is the Coulomb friction level; F_S is the level of the stiction force and v_S is the Stribeck velocity. The function $g(\dot{x})$ need not be symmetrical. Direction dependent behavior can therefore be captured.
The friction force generated from the bending of the bristles is described as (including a term to account for viscous friction)

$$F = \sigma_0 z + \sigma_1 \frac{dz}{dt} + \sigma_2 \dot{x} \tag{2.3}$$

where σ_0 is the stiffness, σ_1 a damping coefficient and σ_2 represents the viscous friction.
The LuGre model is characterized by six parameters: σ_0, σ_1, σ_2, F_C, F_S and v_S. All phenomena mentioned earlier (paragraph 2.1) are captured in the LuGre model.
In Figure 2-6 the friction curve of this model is shown near zero velocity. This curve is acquired by presenting a sine shape velocity signal to the LuGre model. The curve may differ in other simulations.

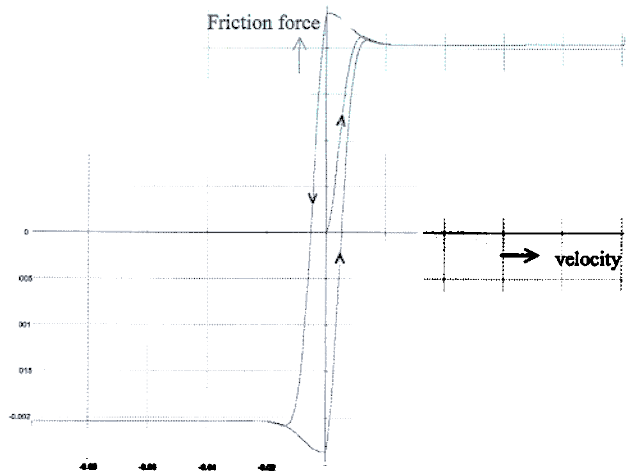

Figure 2-6 LuGre friction curve

2.4 Friction compensation

The performance of a system is generally limited due to the presence of friction. Therefore a friction compensation method is used to improve the performance and eliminate the effects of friction. There are many ways to eliminate the effects of friction. In this section some of these compensation techniques are mentioned. The section is a summary of the techniques discussed in (Spreeuwers, L., 1999). The task of a machine is of importance in order to know which friction phenomenon is dominant. So first the different tasks of a system are discussed.

2.4.1 Compensation tasks

There are different control tasks in which friction compensation may be necessary. These tasks can be divided in four groups: precision positioning, tracking with velocity reversals, low velocity tracking and high velocity tracking. The four tasks are described below and the dominant friction component is mentioned (Armstrong-Hélouvry, B. et al., 1994).

- *Precision positioning*
  Precision positioning is a regulator task. The system spends most of the time near or within the static friction regime. The dominant frictional phenomenon is static friction.
- *Tracking with velocity reversals*
  Tracking with velocity reversals is closely allied with task 1 (precision positioning), due to its frictional cause. As a result of a higher static level of friction, motion through zero velocity is not smooth. A system may pause at zero velocity until sufficient force is applied to exceed the maximum stiction level. The dominant frictional phenomenon is static friction.
- *Low velocity tracking*
  The desired motion by low velocity tracking is of a constant direction and possibly of constant velocity. During this task, when the desired velocity lies on the negative sloped part of the Stribeck curve, stick-slip may occur. The dominant frictional phenomena are the Stribeck effect and static friction.
- *High velocity tracking*
  High velocity tracking is dominated by viscous friction and the Stribeck curve is positively sloped. Usually there are no problems with the stability, but instead the tracking error is observed to increase as a function of velocity

The effectiveness of a particular compensation technique depends on the compensator task, because a certain technique relies on the presence of a certain dominant frictional phenomenon (Armstrong-Hélouvry, B. et al., 1994).
The tasks that describes the control tasks of the FCLS best are *tracking with velocity reversals* and *high velocity tracking.*

2.4.2 Friction compensation techniques

In this section a survey of compensation techniques found in literature is given. The compensation techniques can be classified into four main groups: friction avoidance, non-model-based compensation, model-based compensation and model-free compensation. At the end of this section a more extensive survey of adaptive friction compensators found in literature is given.

Friction avoidance
The first strategy to reduce the influence of friction on a system is the avoidance of friction. This is usually done in the design and development phase of a system. There are different methods available:

- *Selection of appropriate lubricant*
  By selection of an appropriate lubricant, the negative friction effects (like stick-slip (Armstrong-Hélouvry, B., 1991; Armstrong-Hélouvry, B. et al., 1994)) can be reduced.

- *Increase of Stiffness and reduction of inertia*
  The effect of stick-slip can sometimes be eliminated by making the system more stiff and by reduction of the inertia (Armstrong-Hélouvry, B., 1991; Armstrong-Hélouvry, B. et al., 1994).
  Use of special bearings
  Special bearings (like ball bearings, oil or air hydrostatic bearings and non contact active magnetic bearings) can sometimes be used to avoid the nonlinearity of low velocity friction (Armstrong-Hélouvry, B. et al., 1994).
- *Replacement of sliding contacts with rolling contacts*
  Replacing sliding contacts with rolling contacts can reduce the friction (Spreeuwers, L., 1999).

Non-model-based compensation
With non-model-based friction compensation, no model is explicitly used for the design of the friction compensator.

- *High gain PD/PI/PID control*
  A common way of friction compensation is the use of a high gain PD, PI or PID controller (Armstrong-Hélouvry, B. et al., 1994). The bounded non-linear friction can be seen as disturbances that must be cancelled out by the controller. For this compensation technique no characterization of friction is needed, but the use of high gains makes the controller sensitive for high-frequency measurement noise and controller saturation (Altpeter, F. et al., 1997).
- *Fuzzy PI control*
  This technique uses different gains for the different regions of the friction curve. So for low velocities other gains are used than for high velocities. The gains are computed on the basis of the input and output of the system and on the basis of the reference signal (Spreeuwers, L., 1999).
- *Dither and pulse width modulation*
  Dither is a high frequency signal introduced into the system by adding it to the error signal in the feedback loop to smoothen the discontinuity of friction at low velocities. If the frequency is chosen to be higher than the cut-off frequency of the system, the high-frequency behavior is filtered out mostly, leaving only the low-frequency "average" response (Leonard, N.E. and Krishnaprasad, P.S., 1992).
  Pulse width modulation controllers give pulses to the motor (Armstrong-Hélouvry, B. et al., 1994). The principle of this method, as is the case with dither, is averaging of the nonlinearity.
- *Impulsive control*
  With this method a pulse is applied to a system in rest, which result in a small displacement. By making the impulses of great magnitude but short duration, the static friction is overcome and the sensitivity to friction is reduced (Armstrong-Hélouvry, B. et al., 1994).

Model-based compensation

In this group of compensation techniques a friction model is explicitly utilized for the design of the friction compensation. With these techniques is it usually the case that a friction component is calculated and then added to the controller signal. The friction compensator has as an input signal either the reference, measured or estimated velocity (some compensators need besides the velocity also other signals).

- *Fixed compensation*
  Fixed model-based friction compensation uses a compensator with the parameters of the friction model fixed at one value. Once the parameters are estimated through experiments, they are used in the compensator.
- *Robust compensation*
  With a robust model-based friction compensator, the friction parameters do not have to be known exactly. It is assumed that the friction parameters of the friction model used are known within certain bounds.
- *Adaptive compensation*
  In contrast to fixed compensation, the parameters (or some of the parameters) of the friction model used in the adaptive compensator are adaptively updated.
- *Learning compensation*
  Learning model-based friction compensation is a friction compensation method in which the parameters of the friction model are learned.

Model-free compensation

Model-free compensation is model-based compensation without explicitly using a parametric friction model but where, after a certain learning period, a non-parametric friction model is implicitly present within the friction compensator (Spreeuwers, L., 1999).

- *Repetitive compensation*
  In situations where a machine has to carry out a repetitive task, repetitive friction compensation can be applied. A table of corrections for the friction effects is learned during the execution.
- *Learning compensation*
  A learning friction compensator uses no (or a little) a-priori knowledge to determine the friction curve. There are several learning algorithms to learn the friction curve. In this thesis when learning compensation is mentioned this compensation technique is meant.

Adaptive Friction Compensators in Literature

In (Friedland, B. and Park Y.J., 1992) the friction is represented by a force that is a nonlinear, zero-memory, odd-function of velocity. It uses the simplest representation of friction: the Coulomb model. The magnitude (Coulomb friction level) is estimated by a nonlinear reduced-order observer. The simulations discussed in (Friedland, B. and Park Y.J., 1992) show an improvement in the performance of the system. These results are verified in experiments (Amin, J. et al., 1997). And also in experiments the use of this compensator showed an improvement of the performance.

A compensator that includes besides the Coulomb friction also the viscous friction is described in (Canudas de Wit, C. et al., 1987). The friction is parameterized by four parameters, two for positive velocities and two for negative velocities. The four parameters are adapted based on the recursive least square adaptation algorithm. The benefit of this compensator has been demonstrated in experiments on a servo.

In (Bai, E.W., 1997) the friction force is represented by a viscous friction part and a negative viscous (regime 3) + Coulomb friction part. The two parts are parameterized by a model linear in parameters, which are then applied to linear adaptive techniques. Simulations demonstrate an improvement of the performances of the system when the adaptive friction compensation is applied. However, a critical note is given on the use of adaptive friction compensation. An adaptive friction compensator is based on a friction model. If the model is inexact, the friction can be overcompensated. This can lead to limit cycles and in turn impose serious limitations on the closed loop performance.
A comparison of several friction compensation techniques, to improve low-velocity position tracking performance in the presence of velocity reversals, is made in (Leonard, N.E. and Krishnaprasad, P.S., 1992). In this paper three adaptive friction compensators are discussed: two model reference adaptive controllers based on respectively a Coulomb plus viscous friction model and a Stribeck friction model, and an estimation based adaptive controller based on the Dahl model. These compensators are compared through experiments on a dc-motor with an optimized PID controller and a controller with (limited frequency) dither. All the adaptive compensators provide an improved position control compared to the PID and the controller with dither. The estimation based adaptive controller with the Dahl model showed a much better performance then the other adaptive compensators, caused by the fact that the static models used in the model reference adaptive controllers were overcompensating when the friction force changed instantaneously.
In (Feemster, M. et al., 1999) two adaptive controllers are presented. The first adaptive control design is based on a modular approach and incorporates Coulomb, viscous, static and Stribeck friction. Modular controller design implies that the controller is designed to ensure input-to-state stability with respect to the parameter estimation error while the adaptive update laws are used to compensate for the unknown, constant parameters which appear linearly in the model. For the second adaptive friction compensator, using a nonlinearly parameterized Stribeck friction model, a Lyapunov-based adaptive control design procedure has been used. In experiments is shown that these compensators are able to reduce the effects of friction.
The following three adaptive friction compensators are based on the LuGre friction model (Canudas de Wit, C. and Lischinsky, P., 1997; Lischinsky, P. et al., 1999; Panteley, E. et al., 1998). In (Canudas de Wit, C. and Lischinsky, P., 1997) two adaptive compensators are designed (in (Lischinsky, P. et al., 1999) these compensators are implemented on a industrial hydraulic robot), which are based on the adaptation of only one new parameter. In that paper the possibility is investigated to cope with 'structured' friction variations. It is assumed that changes in friction are mainly due to either changes in the normal forces that affect proportionally the static friction characteristics or to temperature changes affecting uniformly both static and dynamic parameters (Canudas de Wit, C. and Lischinsky, P., 1997). For these adaptive compensators it is necessary to have proper initial values for the six friction parameters of the LuGre model. The experimental results presented in (Canudas de Wit, C. and Lischinsky, P., 1997) show that the adaptive compensator improves over a fixed compensation scheme and over a PID controller without friction compensation. This is confirmed in (Lischinsky, P. et al., 1999) by experiments on an industrial Schilling Titan II hydraulic robot.
In (Panteley, E. et al., 1998) an adaptive friction compensator for a n-dof rigid robot manipulator based on the LuGre model is presented. The compensator will not only adapt changes in the friction parameters, but will also adapt the system parameters (in the case of the flight stick the inertia). The LuGre friction model is rearranged in such way that the friction force can be treated as a disturbance. The control signal (controller + compensator

signal) is designed in two steps, first a classical adaptive robot controller that (strictly) passifies the system is used, then a relay-based outer-loop is added that rejects the disturbance (friction). Experiments show an improvement of the performance of a system with friction (although not distinguishable from the controller of (Friedland, B. and Park Y.J., 1992), an adaptive friction compensator based on the Coulomb friction model).

2.5 Adaptive Friction compensation versus Learning Friction compensation

In (Spreeuwers, L., 1999) the conclusion is drawn that (model-free) learning friction compensation seems to be the most appropriate technique for friction reduction when the behavior near zero velocity is of importance. To verify this conclusion learning friction compensation has to be compared to other friction compensation techniques. Since the friction parameters of a system (often) vary during the runtime of the system, adaptive friction compensation seems also suited for the task of reducing the effects of friction. However, there are some drawbacks on the use of adaptive friction compensation. A danger of overcompensation exists when the true friction characteristic is not in the model set (Armstrong-Hélouvry, B. et al., 1994; Bai, E.W., 1997). Adaptive compensation can not deal with parameters appearing nonlinearly in the friction model (as is the case of the LuGre model). In comparison with learning friction compensation, adaptive friction compensation requires more a-priori knowledge, such as the dominant friction phenomena (for a sound choice of the friction model used) and initial parameters (the friction compensator has to work proper from the beginning).
An advantage of adaptive compensation over learning compensation is the ability of adaptive compensation to include some of the dynamic friction phenomena, whereas by learning compensation the friction force is only a static function of the velocity. Dynamic behavior can be included in learning friction compensation, but then different networks are used for different "states" ((Fuzzy) logic state learning friction compensation) (Spreeuwers, L., 1999). So when one (or more) of the dynamic friction phenomena is dominant, adaptive friction compensation is a good option.
On the implementation side the use of learning compensation requires more memory, because all the weights have to be stored, whereas adaptive compensation is only a mathematical equation and therefore requires less memory. The computational power needed for both learning compensation and adaptive compensation depends on the implementation of the compensators: whether the learning compensators updates its weights online or offline; how many splines are used and in which form; which model and update law is used in the adaptive compensator.

3 Design and simulation

In this chapter the adaptive friction compensators are designed and simulated. The control loading system used for these simulations is depicted schematically in figure 3-1. The motor is controlled in a velocity loop with a PI controller. The reference generator calculates the reference velocity from a simulation model, which has as input the applied force. The motor and stick will be modeled as an inertia with friction (LuGre model).

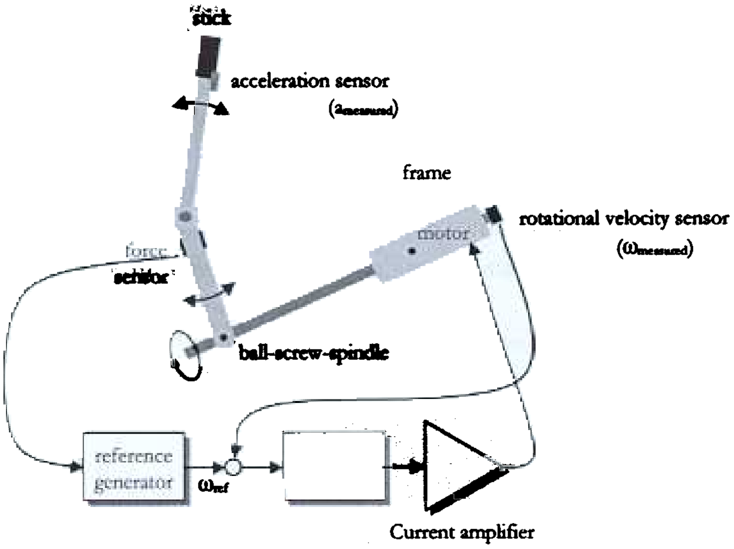

Figure 3-1 Fokker Control Loading System (FCLS)

In this chapter three adaptive friction compensators will be discussed. The first one will use the simplest friction model, i.e. the Coulomb friction model. The compensator is designed to estimate the Coulomb friction level using an observer. The other adaptive friction compensators are based on the LuGre model. Designing an adaptive LuGre model compensator that adapts all the six parameters is difficult if not impossible (Canudas de Wit, C. and Lischinsky, P., 1997). The friction parameters appear nonlinearly in the LuGre friction model. Furthermore the state z is not measurable and to estimate state z it is necessary to know some of the nonlinear parameters. So there is no global solution for this model, therefore it is difficult (impossible) to adapt all the six parameters (Canudas de Wit, C. and Lischinsky, P., 1997). However adaptive friction compensators based on the LuGre model can be found in literature (Canudas de Wit, C. and Lischinsky, P., 1997; Lischinsky, P. et al., 1999; Panteley, E. et al., 1998). The first LuGre based compensator is a modification of the first compensator (Coulomb friction) where the Coulomb friction model is replaced by the LuGre friction model. The other friction compensator is found in literature (Panteley, E. et al., 1998). This adaptive friction compensator adapts four parameters, including the system parameter (inertia of the stick). All the parameters (the six parameters of the LuGre model and the inertia) are assumed to be unknown. The friction is treated as a disturbance.

But before the compensators can be designed and simulated the parameters (inertia and LuGre model) should be identified. This is done in paragraph 3.1. The adaptive friction compensators are then discussed in the subsequent paragraphs. The adaptive Coulomb friction compensator in paragraph 3.2, the adaptive LuGre (1) friction compensator in paragraph 3.3 and finally the compensator that adapts four parameters in paragraph 3.4.

3.1 Identification of the FCLS

In order to design and simulate properly it is necessary to identify the (friction) parameters of the FCLS. The FCLS can be regarded as a moving mass system with friction. The friction model used in the system is the LuGre friction model, because this model incorporates all friction phenomena mentioned in paragraph 2.2. Also the found parameters can be used in the compensators based on the LuGre model. The parameters to identify are the inertia of the motor and the parameters of the LuGre model. For the identification of these parameters, a method of four steps is used, partially based on sheets found on the internet (Canudas de Wit, C., 1998). The four steps are:

1. Identification of inertia J, Coulomb friction (F_c) and viscous friction (σ_2): Gross motion in sliding regime.
2. Identification of Static friction (F_s): Estimation of the breakaway force.
3. Identification of the Stribeck velocity (v_s): Motions at low velocities.
4. Identification of Dynamic Parameters (σ_0 and σ_1): motions in the presliding region.

The process function of the stick can be describes as:

$$J\ddot{x} = u - F$$

with

$$F = \sigma_0 z + \sigma_1 \frac{dz}{dt} + \sigma_2 \dot{x}$$

$$\frac{dz}{dt} = \dot{x} - \frac{|\dot{x}|}{g(\dot{x})} z$$

$$\sigma_0 g(\dot{x}) = F_c + (F_s - F_c)e^{-\left(\frac{\dot{x}}{v_s}\right)^2}$$

This model will be used for the identification of the system parameters (inertia and friction).The four steps will now be discussed.

Step 1: Identification of J, F_c and σ_2

For the identification of J, F_c and σ_2 it is necessary to regard motions much larger then the Stribeck velocity (so the Stribeck effect can be neglected), and there must be a friction steady state behavior ($F \cong F_{SS}$).
The friction model becomes:

$$F \approx F_c \operatorname{sgn}(\dot{x}) + \sigma_2 \dot{x}$$

and the motor model becomes

$$J\ddot{x} = u - F_c \operatorname{sgn}(\dot{x}) - \sigma_2 \dot{x}$$

To each signal a low pass filter ($H(s) = \frac{1}{\tau s + 1}$) will be applied. The control signal then becomes

$$y = \theta^T \varphi$$
with
$$y \triangleq u \tag{3.5}$$
and
$$\theta \triangleq \begin{bmatrix} J \\ \sigma_2 \\ F_c \end{bmatrix}, \text{and } \varphi \triangleq \begin{bmatrix} \ddot{x} \\ \dot{x} \\ \operatorname{sgn}(\dot{x}) \end{bmatrix}$$

The parameters will be estimated with Exponentially Weighted Recursive Least Squares (EWRLS) (Canudas de Wit, C., 1998), that is;

$$\hat{\theta}(k) = \min_{\hat{\theta}(k)} \sum_{i=1}^{k} \lambda(k) \cdot \left(y(i) - \varphi(i)^T \hat{\theta}(k)\right)^2$$
$$\lambda(k) = \eta(\dot{x}(k)) \cdot \lambda^{k-i}, 0 < \lambda \le 1$$
$$\eta(v(k)) = \begin{cases} 1 \text{ if } |\dot{x}(\mathrm{k})| > \dot{x}_{\min} \\ 0 \text{ else} \end{cases}$$

To the FCLS an exponentially increasing force has been applied. In Matlab the acquired data has been analyzed and the three parameters were estimated using the EWRLS method. The results are given in Table 3-1.

Step 2: Identification of F_s

For the identification of the static friction the applied force has been linearly increased. The maximum of the applied force after each step has also been increased. The value of the static friction can be found by estimation of the applied force when the stick is moving away. In Figure 3-2 the applied control signal and position of the motor can be seen. The static friction is overcome when the control signal is about 16e-3 V (which corresponds to a current of 16e-3 A), which corresponds to an applied force of 2.56e-3 N (the motor constant of the FCLS is 0.16 N A^{-1}). The static friction is larger than the Coulomb friction (which is normal in systems).

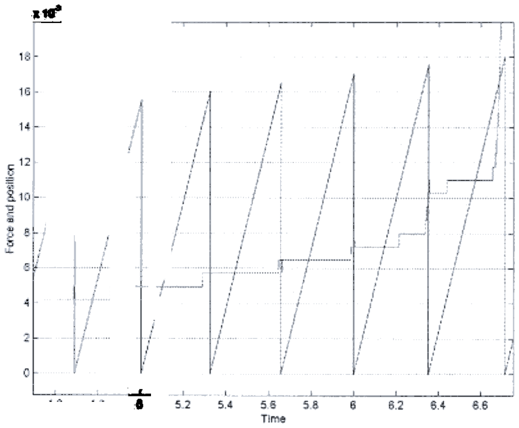

Figure 3-2 Static friction estimation: control signal and position

Step 3: Identification of Stribeck velocity

To estimate the Stribeck velocity it is necessary to have motions at sufficiently small velocity. Then the steady state behavior is:

$$F \approx (F_c + (F_s - F_c)e^{-(\dot{x}/v_s)^2})\operatorname{sgn}(\dot{x})$$

When this expression is substituted in $J(\ddot{x}) = u - F$ (with known J, F_c and F_s), a linear parameterization of the unknown parameter v_s is allowed:

$$\dot{x}^2(t) = v_s^2 \ln \gamma(t),$$
$$y(t) = \theta\varphi(t),$$

with

$$y(t) \triangleq \dot{x}^2(t),\ \theta \triangleq v_s^2,\ \varphi(t) \triangleq \ln\gamma(t)$$

and

$$\gamma \triangleq \frac{F_s - F_c}{(u - J\ddot{x})\operatorname{sgn}(\dot{x}) - F_c},\ F_s > F_c$$

A real solution for v_s only exists if $\gamma \geq 1$. Data violating this condition is removed from the set. The remainder of the data is used to estimate v_s with a least squares estimation. The experiment is done using a standard PI controller. The reference signal was $x_d = A\cos(\omega t)$, with $A << |x_{max}|$. The result can be found in Table 3-1.

Step 4: Identification of σ_0 and σ_1

For the identification of σ_0 motions in the pre-sliding region are regarded, where elastic effects dominate over the plastic effects.

$$F << F_s,\ z \cong 0,\ \dot{x} \cong 0,$$

which implies that $\dot{z} \cong v$, and that

$$F \cong \sigma_0 x + (\sigma_1 + \sigma_2)\dot{x} \cong \sigma_0 x$$

In stiction, $\dot{x}$ is very small and then $u \cong F$. Hence

$$y(t) = \theta\varphi(t)$$
$$y(t) \triangleq u(t),\ \theta \triangleq \sigma_0,\ \varphi(t) = x(t)$$

σ_1 can not be identified directly (according to (Canudas de Wit, C., 1998)). To get well behaved stick-slip transitions during simulation σ_1 can be chosen such that a given damping ζ is imposed. The linear approximated map $G(s): x \mapsto u$ in the pre-displacement region is:

$$G(s) = \frac{1}{Js^2 + (\sigma_1 + \sigma_2)s + \sigma_0}$$

With a given damping, typically $\zeta = 1$, σ_1 becomes:

$$\sigma_1 = 2\zeta\sqrt{\sigma_0 J} - \sigma_2$$

In figure 3-2 (estimation of the static friction) the encoder steps in the position curve can be seen. Since the estimation of the dynamic parameters requires data from the sticking regime (forces smaller than the static friction) the accuracy of the position is not good enough for a proper estimation of the dynamic parameters. So the dynamic parameters has to be guessed. For the simulations σ_0 = *100 [N m rad^{-1}]* and σ_1 = *6e-2 [N m s rad^{-1}]* are used (these values are about the values found in (Canudas de Wit, C., 1998)).
In Table 3-1 the identified parameters are given.

Parameters	Estimation	Assumption
J [kg m^{-2}]	7.8911e-6	-
$F_{Coulomb}$ [N m]	2.0388e-3	-
F_{static} [N m]	2.5600e-3	-
$v_{Stribeck}$ [rad s^{-1}]	9.5633e-3	-
σ_0 [N m rad^{-1}]	-	100
σ_1 [N m s rad^{-1}]	-	6e-2
σ_2 [N m s rad^{-1}]	8.9044e-5	-

Table 3-1 Estimation of system parameters FCLS

The dominant friction phenomena on the FCLS are the static phenomena. The influence of the dynamic phenamena is nil. So a static friction model incorporating the static friction phenomena is sufficient for the FCLS. However, to get insight in the (dynamic) LuGre model for simulations and experiments for other projects where the dynamic phenomena have greater influence on the performance of a system, this model is used in this assignment.
With these values a simulation is done with the PI controller used in all simulations and experiments, without any friction compensation. The model of the stick is depicted in Figure 3-3.

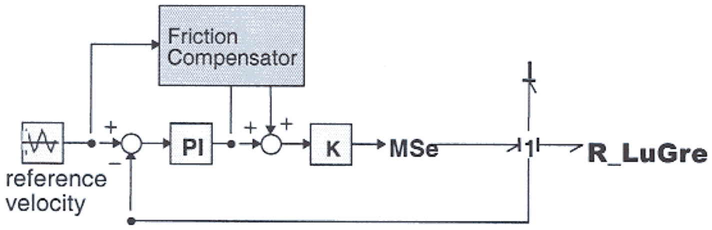

Figure 3-3 Model of the FCLS in 20-sim

The friction compensation part is switch off in order to simulate the behavior of the PI controller. The behavior of the motor near a velocity reversal is given in figure 3-4. The reversal bump can be seen clearly in this simulation.

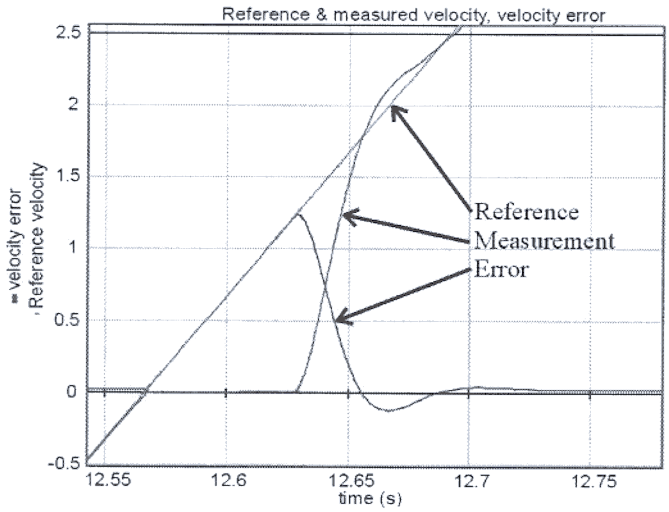

Figure 3-4 Velocity reversal of the standard PI controller

3.2 Adaptive Coulomb Friction compensation

The first adaptive compensator regarded in this thesis has been designed and developed in (Friedland, B. and Park Y.J., 1992). The friction is represented in the compensator by a nonlinear, zero-memory, odd-function of velocity. The friction is modeled as a constant times the sign of the velocity, which is basically a representation of Coulomb friction

$$f(\dot{x},a) = a\,\mathrm{sgn}(\dot{x}) \tag{3.14}$$

where $f(\dot{x},a)$ is the friction force and $\dot{x}$ is the velocity. The dynamics of the process with friction are given by

$$\ddot{x} = -f(\dot{x},a) + w \tag{3.15}$$

where w is the force due to all sources other than friction. The parameter a is to be estimated by an observer. The observer is given in the form of a nonlinear reduced-order observer:

$$\hat{a} = z - k|\dot{x}|^{\mu} \tag{3.16}$$

where the $k > 0$ and the exponent $\mu > 0$ are design parameters and the variable z is given by

$$\dot{z} = k\mu|\dot{x}|^{\mu-1}[w - f(\dot{x},\hat{a})]\operatorname{sgn}(\dot{x}) \tag{3.17}$$

where $w - f(\dot{x},\hat{a})$ is the output of the controller (in case of the FCLS the output of the PI controller).
To study the performance of the observer, the error between the actual parameter a and its estimate $\hat{a}$ has to be regarded. Assuming that the true parameter a is constant, and letting

$$e \triangleq a - \hat{a} \tag{3.18}$$

this becomes

$$\begin{aligned} \dot{e} &= -\dot{\hat{a}} \\ \dot{e} &= -\dot{z} + k\mu|\dot{x}|^{\mu-1}\ddot{x}\operatorname{sgn}(\dot{x}) \\ \dot{e} &= k\mu|\dot{x}|^{\mu-1}\operatorname{sgn}(\dot{x})[\ddot{x} - w + f(\dot{x},\hat{a})] \end{aligned} \tag{3.19}$$

With the use of the process function (3.15) this becomes

$$\begin{aligned} \dot{e} &= -k\mu|\dot{x}|^{\mu-1}\operatorname{sgn}(\dot{x})[f(\dot{x},a) - f(\dot{x},\hat{a})] \\ \dot{e} &= -k\mu|\dot{x}|^{\mu-1}\operatorname{sgn}(\dot{x})[(a-\hat{a})\operatorname{sgn}(\dot{x})] \\ \dot{e} &= -k\mu|\dot{x}|^{\mu-1}, \end{aligned} \tag{3.20}$$

which, for $k > 0$, $\mu > 0$, converges asymptotically to zero if $\dot{x}$ is bounded and away from zero. This compensator can be used in both a feedback and a feedforward mode. The main advantage of the use of the feed forward mode is that the compensator is not (or less) sensitive to (measurement) noise. Since the compensator has a relay function (sign) the noise could give problems when a feedback mode is used. When the reference wants the system to stand still, the reference generates a signal that is zero, but the measured velocity will not actually be zero, due to the noise. For the relay based compensator it does not matter whether the velocity is (very) low or high. The compensator compensates the friction with maximum output. This can lead to instability of the stick. So for the simulations and the experiments a feed forward mode will be used.
The adaptive Coulomb friction compensator has been implemented in 20-sim. The model is given in figure 3-4.

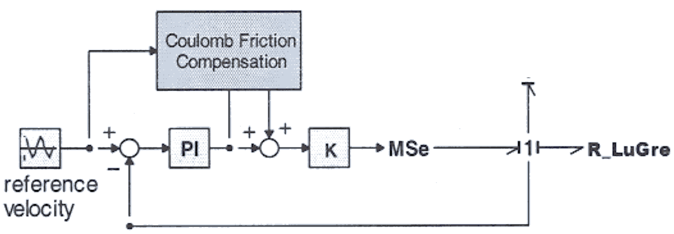

Figure 3-5 Model of Adaptive Coulomb Friciton Compensator and the FCLS

The parameters of the process (inertia and friction) are chosen according to Table 3-1. The first simulation is to examine whether the adaptive parameter will converge. The result of this simulation is given in Figure 3-6. For various initial values of z the curve of a_{est} is given (the reference is a sine shaped signal).

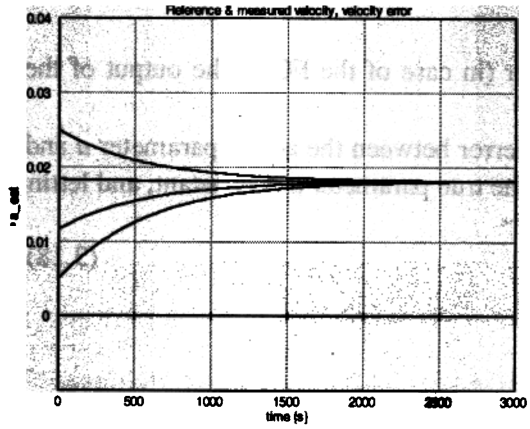

Figure 3-6 Convergence of a_{est} for various $z(0)$

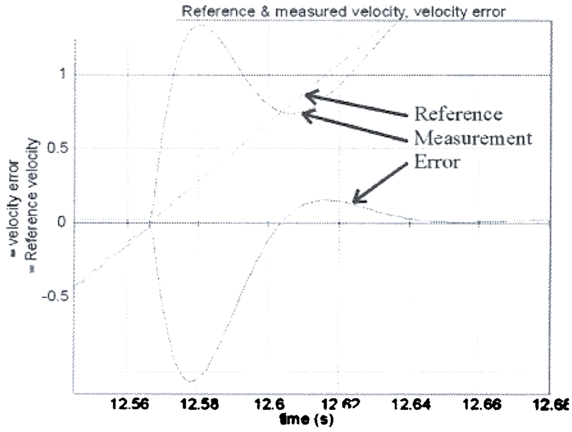

Figure 3-7 Velocity error of Coulomb friction compensator

From Figure 3-6 it is clear that the adaptive parameter a_{est} converges for these situations. The value to which a_{est} converges ($a_{est} \cong 0.018$) is used in a simulation to examine the reversal bump. In Figure 3-7 the velocity reversal of this simulation is given. The reversal bump is replaced by an overcompensated reversal bump. The amplitude of the error has the same magnitude as the error of the PI controller during a velocity reversal. The cause for this is a too high value of a_{est},, which is due to the fact that the observer minimizes the error for the whole range of the velocity and not only for the reversal bump. Besides this the friction model used in the compensator is not like the true friction (which is in this case the LuGre model). So the disadvantage of adaptive compensation is that when a model used in the compensator is not like the true friction the danger exists that there will be overcompensation. There are several solutions for this problem:

1. To smoothen the relay function, i.e. to replace the sign function with the tanh function. With this function the compensation force is slowly build up and this will reduce the overcompensation.
2. The friction phenomenon of interest for the reduction of the reversal bump is the static friction. The static friction is only of importance in a small region round zero velocity. So to compensate only for the static friction the observer should only update itself in a region around zero, and minimize the error introduced by the static friction.

Both solutions have been implemented on the friction compensation. The introduction of a limited update region results in a reduction of a_{est} ($a_{est} \cong 0.0137$, and actually represent a Coulomb friction force of 2.192e-03 [Nm], a more realistic estimation of the Coulomb friction force (2.0388e-03 [Nm]). In Figure 3-8 and Figure 3-9 simulations of the new compensator are depicted. The *sign* function of (3.14) is replaced by a *tanh* function ($sign(\dot{x}) \Rightarrow tanh(k\dot{x})$, with k the gain and $\dot{x}$ the velocity). In Figure 3-8 gain k is 1000, which makes the tanh function practically the same as a sign function, but continuous and in Figure 3-9 gain k is 10. In both simulations the region where the observer is allowed to update itself (the velocity margin) is set to 4. Outside this margin the effects of the velocity reversal are minimal.

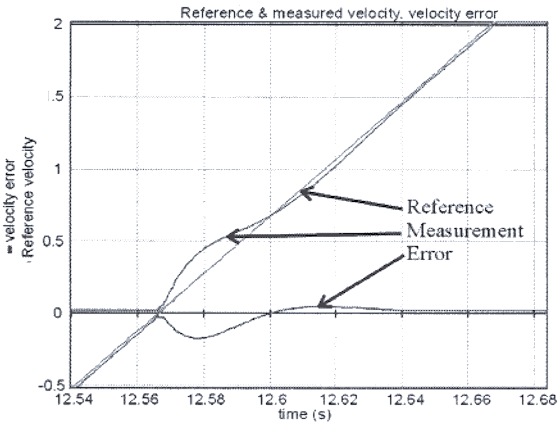

Figure 3-8 Velocity reversal: limited update Coulomb friction compensation with tanh (v = 4; gain = 1000)

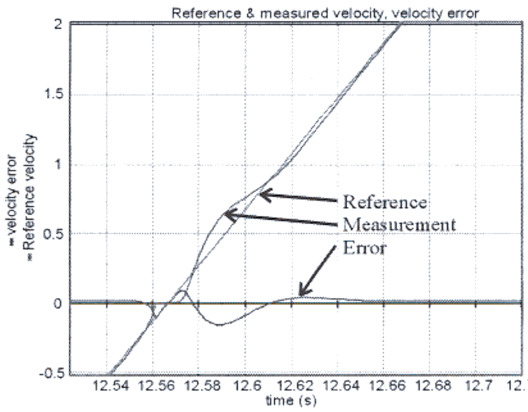

Figure 3-9 Velocity reversal: limited update Coulomb friction compenasation with tanh (v = 4; gain = 10)

The error is reduced by a factor 6 for both compensators. However, in case of a gain of 10 the stick is sticking instead of being overcompensated, so there should be an optimal gain between 10 and 1000 where the error is minimized.
This compensator (with the suggested adjustments) is able to reduce the reversal bump significantly, even though the used friction model is simple and not like the true friction (in case of the simulations the LuGre friction model).

3.3 Adaptive LuGre (1) Friction compensation

The adaptive LuGre (1) friction compensation is derived from the adaptive Coulomb friction compensation. Instead of the sign function (or tanh function in the adjusted compensator), which represent the Coulomb friction, the LuGre friction model is used. The compensator will have the following structure (the same representation of the process from the previous paragraph does apply):

$$\begin{aligned} f(\dot{x},\hat{a}) &= \hat{a} * F_{\text{LuGre}}(\dot{x}) \\ \hat{a} &= m - k|\dot{x}|^{\mu} \\ \dot{m} &= k\mu|\dot{x}|^{\mu-1}[w - f(\dot{x},\hat{a})]\operatorname{sgn}(\dot{x}) \end{aligned} \tag{3.21}$$

with for F_{LuGre}:

$$\begin{aligned} F_{\text{LuGre}} &= \sigma_0 z + \sigma_1 \frac{dz}{dt} + \sigma_2 \dot{x} \\ \frac{dz}{dt} &= \dot{x} - \frac{|\dot{x}|}{g(\dot{x})} z \\ \sigma_0 g(\dot{x}) &= F_c + (F_s - F_c) e^{-\left(\frac{\dot{x}}{v_s}\right)^2} \end{aligned} \tag{3.22}$$

Using the same derivation as with the adaptive Coulomb friction compensator the performance of this observer becomes:

$$\dot{e} = -k\mu|\dot{x}|^{\mu-1}\,\text{sgn}(\dot{x})[(a-\hat{a})F_{\text{LuGre}}]$$

$$\dot{e} = -k\mu|\dot{x}|^{\mu-1}[\text{sgn}(\dot{x})F_{\text{LuGre}}]e$$

The term $sgn(\dot{x})F_{\text{LuGre}}$ is most of the times a positive number (see for a plot of the F_{LuGre} Figure 2-6), only in a (very) small region around zero velocity the term is negative, which means that the error will not converge in this small region. Outside this region the error converges asymptotically to zero if $\dot{x}$ is bounded and away from zero, and $k > 0$, $\mu > 0$. When the desired velocity is not bounded to a region near the small region where $sgn(\dot{x})F_{\text{LuGre}}$ is negative, this compensator should be able to handle the friction phenomena without divergence of the error. The main disadvantage of this compensator is that the LuGre parameters should be well known, or at least the relative size of the parameters.

This compensator has been simulated in 20-sim. When the values of the parameters of the true friction (R_LuGre in figure 3-4) match the values of the compensator, the velocity error is negligible, i.e. the reversal bump disappears. However, this situation will never occur during the experiments, so the compensator has to be tested on the ability to cope with variations of the parameters. When the true parameters differ from the compensator parameters the error is not zero anymore and the error at velocity reversal is the largest. However since the true parameters of the stick (there is only an estimation of the static parameters: the dynamic parameters are unknown and guessed) are not exactly known it is difficult to predict the behavior of this compensator in the experimental setup.

3.4 Adaptive LuGre (4) Friction compensation

Unlike to the LuGre based compensator discussed in the previous paragraph, the compensator found in (Panteley, E. et al., 1998) assumes all the parameters, including the system parameters (in case of the flight stick the inertia) to be unknown. The compensator is based on the consideration that the initial bristles deflection is bounded (Canudas de Wit, C. et al., 1995),

$$|z(0)| \leq \Delta \hat{=} F_s$$

With this it is ensured that the bristles deflection is uniformly bounded ($|z(t)| \leq F_s/\sigma_0$, for all $t \geq 0$) (Panteley, E. et al., 1998). This is a fundamental property of the model that is used with the development of the compensator. For the development of the adaptive compensator the LuGre friction model has been rearranged in such way that the friction force can be treated as a disturbance. The friction force can be rewritten as follows:

$$F = [\sigma_0 - \sigma_0\sigma_1 g(\dot{x})]z + (\sigma_1 + \sigma_2)\dot{x}$$

Using inequality (3.22) and the inequality $g(\dot{x}) \leq (1/F_c)|\dot{x}|$, which follows from the LuGre model, the first term of F can be bounded as

$$\begin{aligned} |F_d(\dot{x},z)| &\hat{=} |[\sigma_0 - \sigma_0\sigma_1 g(\dot{x})]z| \\ &\leq \Delta + \frac{\Delta}{F_c}\sigma_1|\dot{x}| \end{aligned} \qquad (3.26)$$

The second term of F can be parametrized in the form

$$(\sigma_1+\sigma_2)\dot{x}=Y_2(\dot{x})\theta_2 \tag{3.27}$$

with $Y_2(\dot{x}) = \dot{x}$ and $\theta_2 = \sigma_1 + \sigma_2$. The total friction force can be decomposed as

$$F=F_d(\dot{x},z)+Y_2(\dot{x})\theta_2 \tag{3.28}$$

where F_d will be treated as a linearly bounded disturbance. The control signal consists of two parts

$$u=u_1+u_2 \tag{3.29}$$

where u_1 solves the adaptive global tracking problem for a standard robotic system with viscous friction $Y_2(\dot{x})\theta_2$, and u_2 is added to compensate $F_d(\dot{x},z)$.
For u_1 an adaptive controller is proposed which is described in (Slotine, J.J.E. and Li, W., 1987). The controller is based on sliding mode control. So u_1 can be described as (θ_1 and Y_1 represent the system parameter adaptation)

$$u_1=-K_d d+Y_1(\ddot{x}_d,\dot{x},\dot{x}_d)\hat{\theta}_1+Y_2(\dot{x})\hat{\theta}_2 \tag{3.30}$$

with K_d the controller parameter, $Y_1(\ddot{x}_d,\dot{x},\dot{x}_d)=\ddot{x}_d-\lambda\dot{\tilde{x}}$ and θ_1 = J. The first term of the regressor ($\ddot{x}_d-\lambda\dot{\tilde{x}}$) is derived in (Slotine, J.J.E. and Li, W., 1987) by using the Lyapunov stability for the controller design. The term $\ddot{x}_d-\lambda\dot{\tilde{x}}$ can be seen as virtual 'reference trajectory' (Slotine, J.J.E. and Li, W., 1987). Variable d is defined as (with x the position)

$$\begin{aligned} d &\triangleq \dot{\tilde{x}}+\lambda\tilde{x} \\ \tilde{x} &\triangleq x-x_d \end{aligned} \tag{3.31}$$

and λ and K_d are positive numbers. The update-law for parameters $\hat{\theta}_i$, $i=1,2$ is

$$\begin{aligned} \dot{\hat{\theta}}_1 &= -\Gamma_1 Y_1(\ddot{x}_d,\dot{x},\dot{x}_d)d \\ \dot{\hat{\theta}}_2 &= -\Gamma_2 Y_2(\dot{x})s \end{aligned} \tag{3.32}$$

where Γ_1 and Γ_2 are positive numbers. Together with the error equation

$$J\dot{d}+K_d d=\left[Y_1(\ddot{x}_d,\dot{x},\dot{x}_d),Y_2(\dot{x})\right]\begin{bmatrix}\tilde{\theta}_1\\ \tilde{\theta}_2\end{bmatrix}+u_2-F_d(\dot{x},z)$$

with $\tilde{\theta}_i \triangleq \hat{\theta}_i-\theta_i$ for the parameter error, the update-law defines a map $\Sigma:[u_2-F_d(\dot{x},z)]\to d$, which is *output strictly passive*. This means that there exists constants $\alpha > 0$ and $\beta_1 \in \Re$ such that for all $t \geq 0$

$$\langle u_2-F_d(\dot{x},z)|d\rangle_t \geq \alpha\|d\|_{2t}^2+\beta_1$$

where $\langle x|y\rangle_t \triangleq \int_0^t x(\tau)^T y(\tau)d\tau$ and $\langle x|x\rangle_t = \|x\|_{2t}^2$.

A property of strictly passive systems has been exploit. Strictly passive systems have "infinite gain margin" (Panteley, E. et al., 1998). The suggestion is made to choose u_2 as a *relay-based high gain* feedback that has to eliminate the effect of the "disturbance" $F_d(\dot{x},z)$. So u_2 can be defined as

$$u_2 = Y_3(\dot{x},d)\hat{\theta}_3 \tag{3.35}$$

with

$$Y_3(\dot{x},d) \triangleq -[sign(d), |\dot{x}|sign(d)]$$
$$\dot{\hat{\theta}} = -\Gamma_3 Y_3(\dot{x},d)d$$

The final adaptive controller will be defined as:

$$u = -K_d d + \Phi\hat{\theta} \tag{3.37}$$

with the regressor vector given by

$$\begin{aligned}\Phi &\triangleq [Y_1(\ddot{x}_d, \dot{x}, \dot{x}_d), Y_2(\dot{x}), Y_3(\dot{x},d)] \\ \Phi &\triangleq [\ddot{x}_d - \lambda\dot{\tilde{x}}, \dot{x}, -sign(d), -|\dot{x}|sign(d)]\end{aligned} \tag{3.38}$$

The update-law of the parameter vector is given by

$$\dot{\hat{\theta}} = -\Gamma\Phi^T d,\ \Gamma = \Gamma^T > 0 \tag{3.39}$$

The initial values of θ are given by

$$\theta_{ini} = \begin{bmatrix} J \\ \sigma_1 + \sigma_2 \\ \sigma_0 F_s \\ \dfrac{\sigma_0\sigma_1 F_s}{F_C} \end{bmatrix}$$

This compensator has been implemented in 20-sim. The simulations of this compensator is done with the values for the parameters from (Spreeuwers, L., 1999). With the found parameters of the stick the simulations required to much time (several days). With the parameters found in (Spreeuwers, L., 1999) the working and performance of the compensator is shown in simulations. With the initial values of θ set to the expected values the compensator eliminates the reversal bump. The simulations are also carried out with the initial values of θ set to zero. In Figure 3-10 the evolution of the parameters are shown.

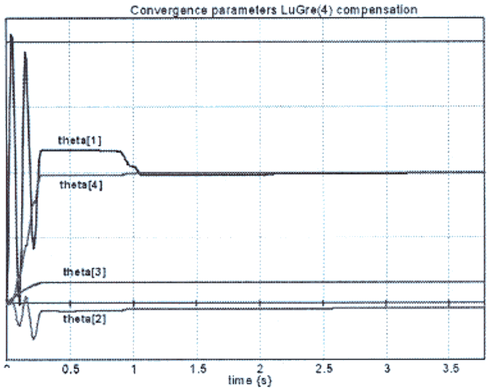

Figure 3-10 Convergence of the parameters (from zero) of the adaptive LuGre (4) compensator

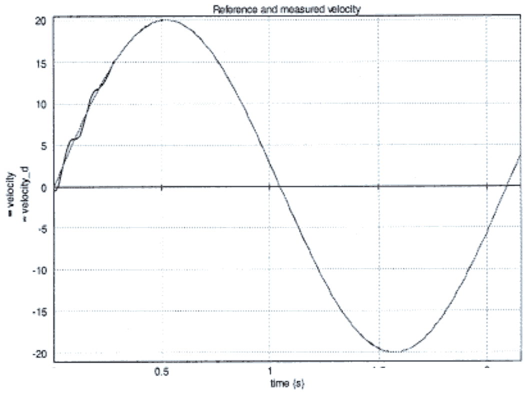

Figure 3-11 Reference and measured velocity of the adaptive LuGre (4) compensator (initial values zero)

After some time the values of the parameters are settled. However the value of the parameter vector θ evolves to a different value than the expected value. The compensator is stuck in a local minimum. Nevertheless from Figure 3-11 can be seen that after a while, when the parameters are settled, the velocity error is small. The reversal bump is also eliminated, as is the case with the expected values of θ. In simulations this compensator looks fine with the parameters of (Spreeuwers, L., 1999), but how this compensator will perform with the identified parameters is not known. This has to be determined in the experiments.

4 Experiments

In this chapter the results of the experiments are discussed. The experiments has been performed on the control loading system of Fokker. The designed compensators of chapter 3 have been implemented on a software platform called 20-works. This is a software framework where the controllers can easily been implemented. The controllers and compensators are made in an agent-based structure (Breemen, A.J.N., 1999), which is integrated in 20-works. The control loading system is controlled with the mentioned software running on a personal computer with an IO-card. In the first paragraph the setup of the system will be described. Paragraph 4.2 deals with the system without friction compensation. In paragraph 4.3 the experiments on the system with learning friction compensation are handled. The adaptive Coulomb, LuGre (1) and LuGre (4) friction compensators will be delt with in paragraph 4.4, 4.5 and 4.6 subsequently. In paragraph 4.7 an overview of the result will be given and a comparison will be made.

4.1 Setup of the system

The experiments have been conducted on the Fokker Control Loading System available on the Control Laboratory. This system is controlled with a PC on which the software is running. The controllers are implemented in the 20-works framework, using an agent-based structure. Only the compensators are newly implemented; the other software parts (reference, actuator and sensor objects) were reused from (Spreeuwers, L., 1999). Of the FCLS, the motor position is measured with an encoder and the motor velocity is measured with a tacho sensor. The adaptive compensators are tested with a reference signal with a constant acceleration (velocity is a saw tooth signal). To test whether the reversal bump is reduced sufficiently (beneath the level of perception) the stick is tested in simulation mode (i.e. with a model consisting of mass only and with use of the force loop).
The compensators are embedded in the agent-based structure of Figure 4-1. The safeguard is added to make sure that the stick does not hit the sides. The normal operation controller consists of a velocity PI controller and the adaptive friction compensator.

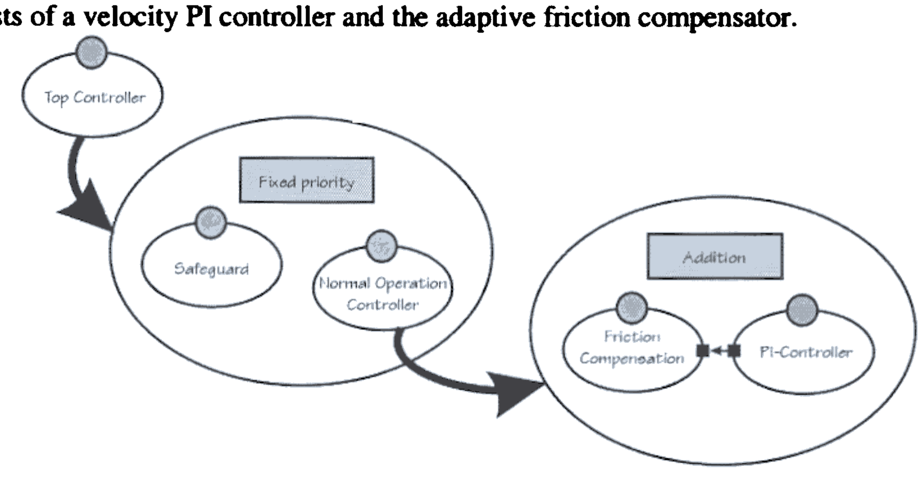

Figure 4-1 Agent-based implementation of the friction compensation

4.2 System without friction compensation

First the system will be tested without any (explicit) friction compensation. The experiments will be carried out using the 'standard' velocity PI controller of (Spreeuwers, L., 1999). This PI controller will be used in all further experiments. The reference signal that will be used during all experiments is depicted in Figure 4-2 (in terms of stick angle).

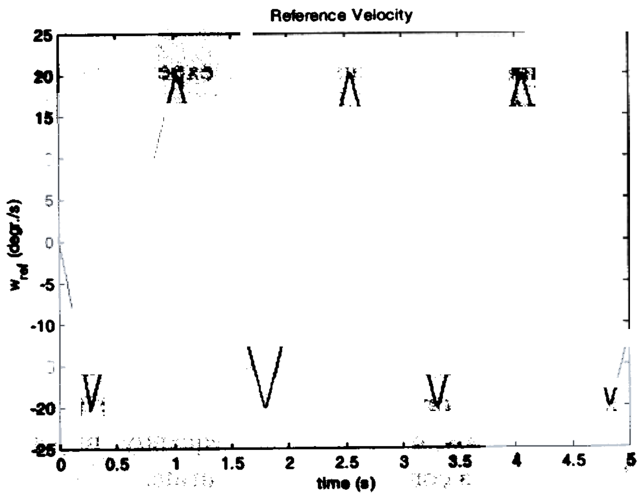

Figure 4-2 Reference velocity for all experiments

When this reference signal is applied the response of the system around zero velocity is given in Figure 4-3.

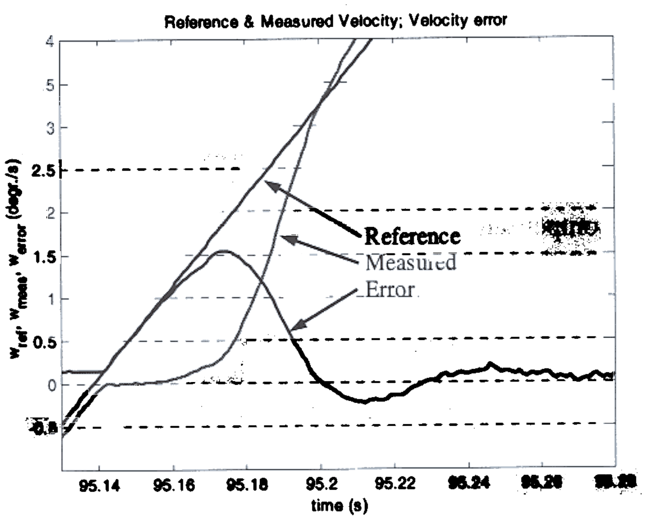

Figure 4-3 Zoom of a velocity reversal without friction compensation

In this plot the problem that arises at velocity reversals can be seen clearly. At zero velocity the systems gets stuck because of the friction. This error, the reversal bump, can be felt when the stick is in simulation mode. The small irregularities in the velocity error signal after the bump are caused by the torque ripple of the motor and the spindle irregularities.

4.3 System with learning friction compensation

In (Spreeuwers, L., 1999) several learning feed forward friction compensators (LFFFC) have been designed and implemented. Two of them, the 'standard LFFFC' and the 'two-distribution LFFFC' accomplished a major reduction of the reversal bump. These two learning compensators will be compared to the adaptive compensators designed in chapter 3. In order to compare the compensators, the learning compensators have to be tested under the same circumstances as the adaptive compensators. So the same reference signal and the same PI-controller are used. The setup of the experiments can be found in appendix B. The reversal bump behavior of the learning friction compensators is depicted in Figure 4-4 and Figure 4-5. The standard LFFFC is able to reduce the reversal bump significantly, by a factor 9. The two distribution LFFFC however gives only a reduction of a factor 3.

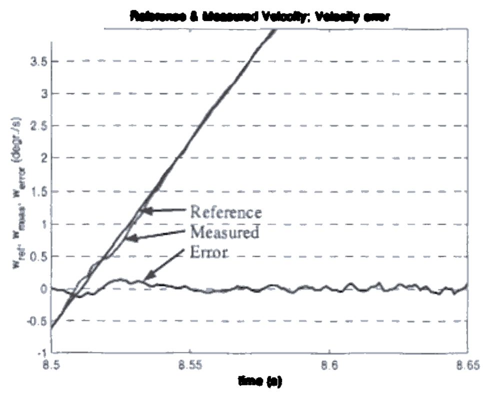

Figure 4-4 Zoom of a velocity reversal with standard LFFFC

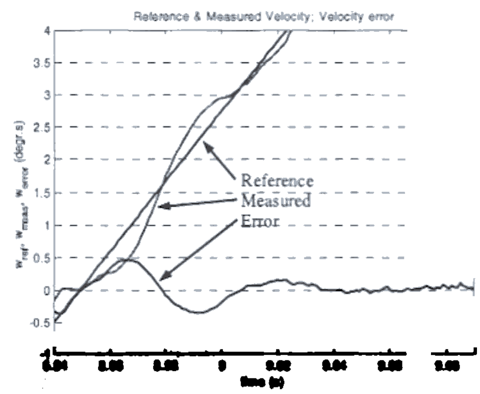

Figure 4-5 Zoom of a velocity reversal with two-distribution LFFFC

4.4 System with adaptive Coulomb compensation

In this section the adaptive Coulomb friction compensation will be tested through experiments. First the observer containing the sign function will be tested on the control loading system. In simulations the convergence of the estimated Coulomb level a_{est} (see Figure 3-6) was shown. This test is also performed on the FCLS and the result is given in Figure 4-6.

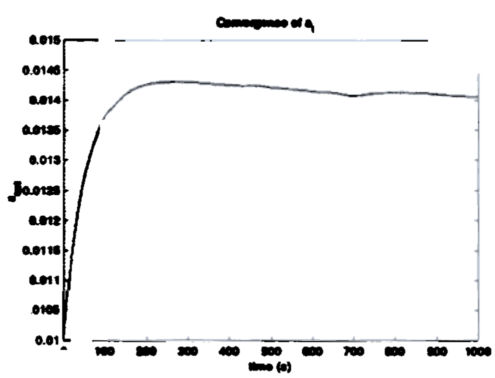

Figure 4-6 Convergence of a_{est}

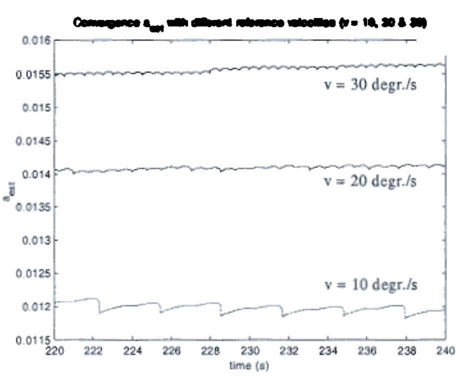

Figure 4-7 Convergence of a_{est} with different reference velocities

In this figure the convergence of a_{est} is demonstrated. The value of a_{est} evolves to about 0.014. This value will be used as initial value for z (which represents the start value of a_{est}). This value for a_{est} differs a little from the simulation (0.014 in experiments to 0.018 in simulations). The evolution of a_{est} is speeded up by a factor 100000 in the integration of z (else the experiments to examine to which value a_{est} evolves took to long). The value of a_{est} is dependent on the velocity set in the reference, see Figure 4-7. When the (reference) velocity reaches higher levels the estimated Coulomb friction level is also higher, which means that the viscous friction is of importance in the system.
The velocity error around zero velocity with this compensator and initial value is depicted in Figure 4-8.

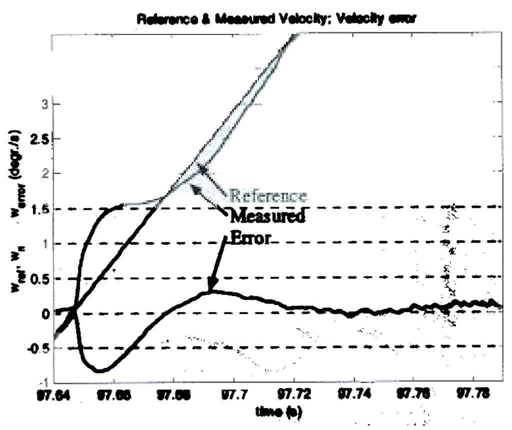

Figure 4-8 Zoom of the velocity reversal with Coulomb friction compensation with sign function

The same problem as with the simulation occurred. Instead of the system getting stuck at zero velocity, the stick is overcompensated and 'swung away'. The resulting error is smaller than the error with the controller without friction compensation. But the reversal bump is not reduced sufficiently: the bump can still be felt and a tick is hearable (which is not the case when no compensation is used). The adjustments suggested in paragraph 3.2 to cope with this problem are also implemented on the FCLS. One extra adjustment has been made in addition to the two adjustments mentioned in paragraph 3.2. During the identification of the LuGre model parameters one experiment was carried out in open loop configuration, when a sine shaped function was applied to the system. The stick was not moving around a constant point, but was drifting away. This effect can have two causes. First the gravity will have its effect on the FCLS. Second the friction can be direction dependent. Because no additional compensators (e.g. for gravity) are implemented, the friction compensator will compensate for this effect. In one direction the gravity will reduce the force required to overcome the Coulomb friction, in the opposite direction the gravity will increase the force required to overcome the Coulomb friction. This give rise to the idea that the Coulomb friction level for both directions is different, so different a_{est} should be used to compensate for the Coulomb friction. This conclusion has been verified in experiments, where an a_{est} is estimated for positive velocities and another a_{est} for negative velocities. In Figure 4-9 the curve of both parameters is shown.

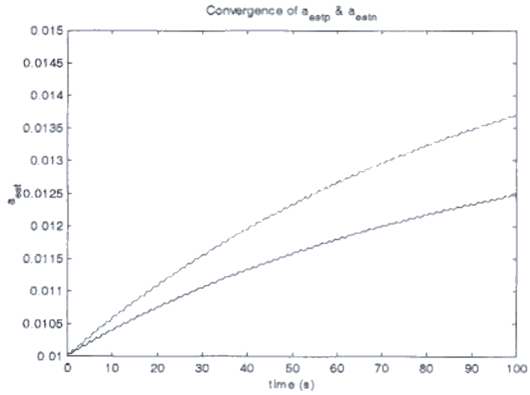

Figure 4-9 Curve of a_{est} for two directions

The two parameters evolve to other values, both around 0.014, so the use of two parameters is justified. However the difference between the two parameters is little and marginal in the reduction of the error. In further experiments (with the Coulomb friction compensator) the compensators exists of two observers (for both directions), although only the velocity error of the one for positive velocities is shown in the figures.

All the adjustments, a *tanh* function instead of a *sign* function, a limited update around zero velocity and two parameters for the two directions, are implemented for the following experiments. For the limited update a velocity margin of 4 is chosen (within this margin the effects of the reversal bump are still noticeable). The value where a_{est} converges to is smaller then when no margin is used (a_{est} converge to 0.011). The velocity error of this compensator (the factor of *tanh* is still 1000, so the *tanh* represents a *sign* function) is given in Figure 4-10.

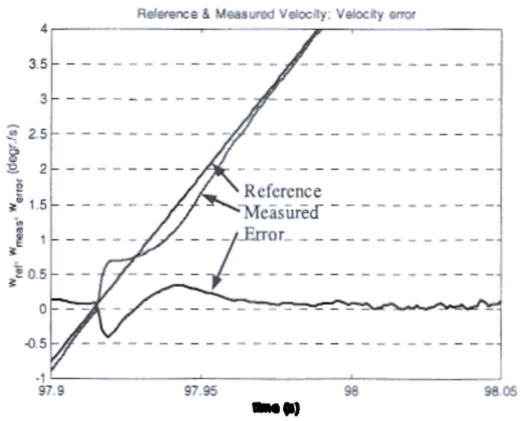

Figure 4-10 Zoom of velocity reversal of the compensator with a velocity margin

The reversal bump is reduced, but a small tick is still hearable. So the desired reduction of the reversal bump is still not accomplished. The friction compensator still overcompensates for the friction (stick is 'swung away'), so the factor of *tanh* could be adjusted in order to smoothen the friction model and reduce the overcompensation.

To estimate a proper value for the factor in the *tanh* function the reversal bump for different factors (1, 10, 100 and 1000) is depicted in Figure 4-11.

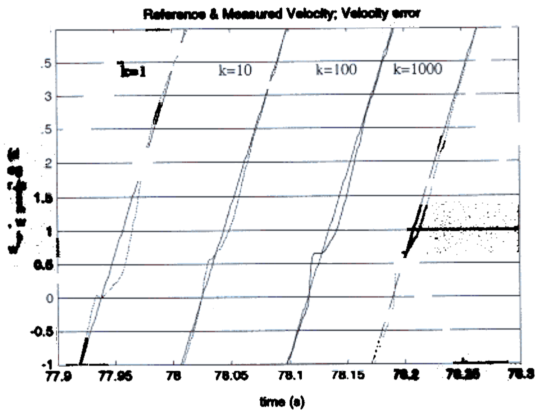

Figure 4-11 Reversal bump versus the factor of *tanh* (from left to right: 1, 10, 100 and 1000)

From this picture can be seen that the transition between overcompensation and sticking at zero velocity is somewhere between factor 1 and 10. To give a more accurate value for the factor, where the error (reversal bump) is minimal, the figures given in Figure 4-12 are showing the velocity reversals for the values between 1 and 10.

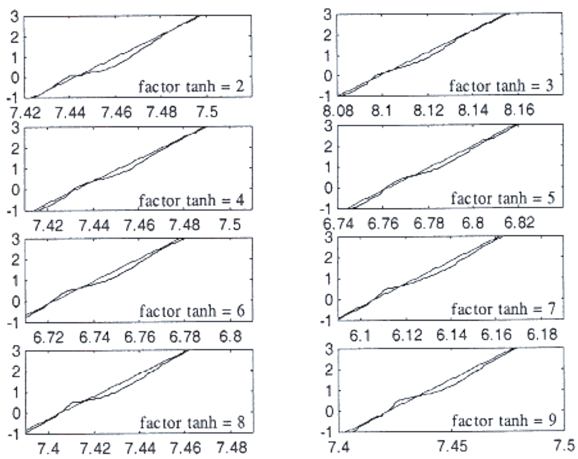

Figure 4-12 Velocity error for different factor *tanh*

The 'best' value for the factor of *tanh* is around the 4. When this factor is used the velocity error around a velocity reversal becomes like Figure 4-13.

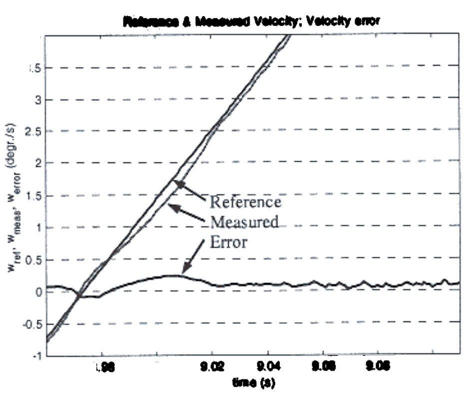

Figure 4-13 Zoom of the velocity reversal of the Coulomb friction compensator with all adjustments

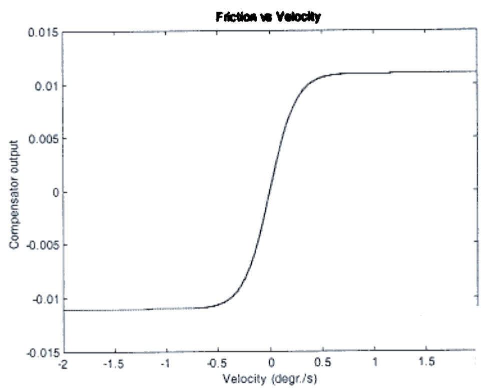

Figure 4-14 Friction versus velocity curve

With this compensator the reversal bump is reduced by a factor 7 in regard to the PI-controller without friction compensation (it is difficult to compare both error signals, because one is obtained when the system is stuck at zero velocity, and this error is clearly the reversal bump and has the highest amplitude, whereas in case of overcompensation the error is small when the actual reversal occur but is larger after some time ('the top' of the error signal)). In regard to the learning friction compensation the error ('the top') is a little bit larger, but this error can not be felt. When this compensator is used in simulation mode the reversal bump can not be felt anymore (although this criterion is subjective). The (hearable) tick which was present during previous experiments is not present anymore with this compensator. The friction curve of the compensator for low velocities is given in Figure 4-14, for high velocities the *tanh* function becomes 1 and so the output of the compensator becomes the Coulomb level (a_{est}).

Although the error at velocity reversals is reduced and can not be felt, velocity errors at high velocities are still present. For both the adaptive and learning compensator the velocity error is given in Figure 4-15 and Figure 4-16. The error at high velocities is for the adaptive compensator (Figure 4-15) the same as for the PI controller without friction compensation, which is comprehensible because the compensator has no (or little) influence on the high velocity characteristics of the total controller. However the high velocity error increases when a learning friction compensator is used (the same applies for the two distribution LFFFC, the error seems even worse), even though the compensator incorporate some viscous friction (Spreeuwers, L., 1999).

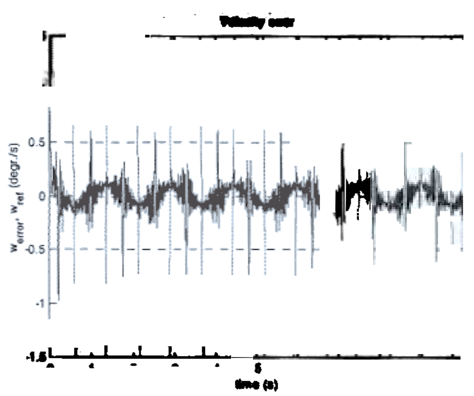

Figure 4-15 Total veloctiy error adaptive Coulomb friction compensation

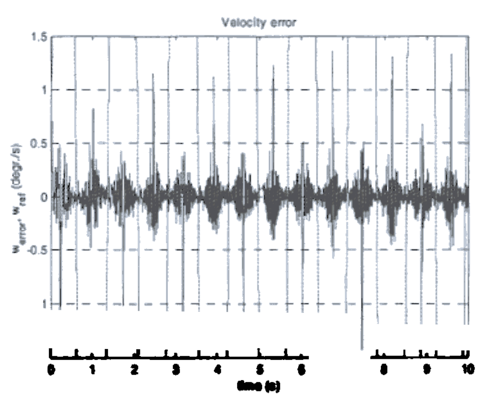

Figure 4-16 Total velocity error of standard LFFFC

In order to reduce the high velocity error a viscous friction compensator can be added. A second observer is added to the compensator to estimate the viscous friction. The observer is the same as used for the estimation of the Coulomb friction level. The result of this addition can be found in Figure 4-17. The viscous friction compensator has no influence on the reduction of velocity error. The performance of the PI controller is of greater importance for the reduction of the high velocity error than a viscous friction compensator. A better alternative for reduction of the high velocity error is the modification of the gains of the PI controller, because the gains of the PI-controller were deliberately set low to assure more stability and gain insight in the robustness of the friction compensator (Spreeuwers, L., 1999). When the gains accidentally were switched the performance of the total controller improved, see Figure 4-18. So if the performance is of interest an optimal PI controller should be used together with the friction compensation.

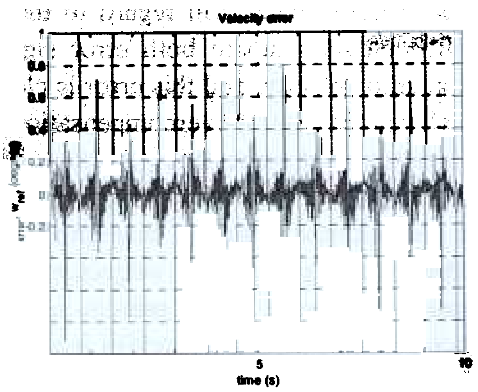

Figure 4-17 Velocity error of controller with adaptive Coulomb and viscous friction compensation

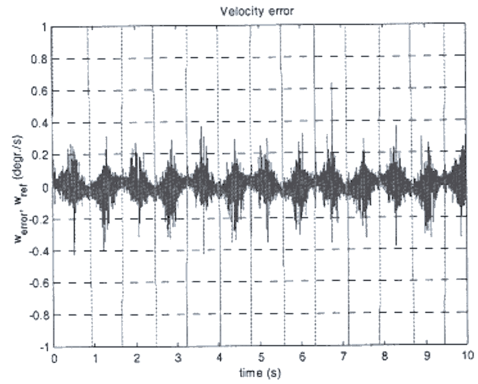

Figure 4-18 Velocity error of controller with modified gains for the PI controller

4.5 System with adaptive LuGre (1) compensation

The second adaptive friction compensator, the adaptive LuGre (1) compensator will be tested in this section. In simulation this compensator eliminated the reversal bump completely when the real friction behaves like the LuGre friction model with known parameters. However, the real friction can never be exactly known so it is important to know how robust the compensator plus controller is. Furthermore, the dynamic parameters of the LuGre model (σ_0 and σ_1) could not be identified for the FCLS, so these parameters has to be estimated on the basis of values found in literature.
The adaptive Coulomb friction compensator of the preivous section has been modified, by replacing the *tanh* (or *sign*) with the LuGre friction description. The parameters of the LuGre model are those of Table 3-1. For the description of the experiments see appendix B. In Figure 4-20 the result of the experiment with the adaptive LuGre (1) friction compensator is given. From this figure it can be seen that initially the reversal bump is reduced significantly (the period of sticking is small) but the compensator then compensates too much, consequently the error is increasing. In Figure 4-21 the friction versus velocity curve is shown. The bump on this curve introduces the increasing error of Figure 4-20. The perpetrator of the bump on the curve is the integration method for the LuGre model. The integration method used in this experiment is given in Figure 4-19.

```
I       = I_next;
I_next  = tame_I * I + ((K*sample_time) / tau_I) * Idot;
I_next  = ( (I_next < -anti_windup) ? -anti_windup : I_next );
I_next  = ( (I_next > anti_windup) ? anti_windup : I_next );
```

Figure 4-19 C++ code of integration method used for the adaptive LuGre (1) friction compensator

With this integration method the LuGre model gets unstable for too high values of the dynamic parameters ($\sigma_0 = 3$) or high velocities. This method is not suitable for computing the LuGre model with a sampling rate of 1000 Hz.

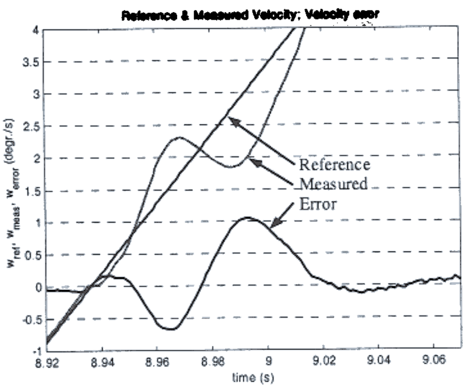

Figure 4-20 Zoom of velocity reversal with adaptive LuGre (1) friction compensation

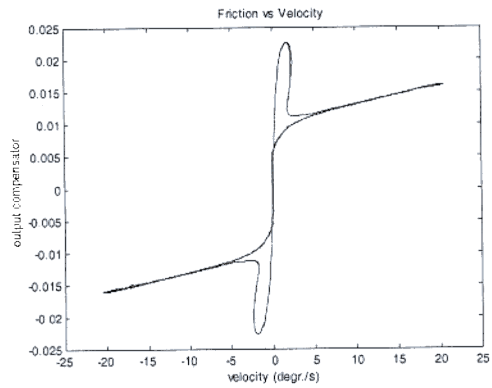

Figure 4-21 Friction compensation versus velocity of adaptive LuGre (1) friction compensation

As is the case with the adaptive Coulomb friction compensator, this compensator also has the tendency to overcompensate for the friction. However, for the adaptive LuGre (1) friction compensator the reason for the overcompensation is (in this case) the integration method for the LuGre model. Nonetheless, the same adjustment as for the Coulomb friction compensator is made for the LuGre (1) friction compensator. In order to get the 'best' value for a_{est} to reduce the reversal bump, the observer is only allowed to update the adaptive parameter in a region around zero velocity. In Figure 4-22 a velocity reversal of the system with the suggested adjustment is depicted, with an accompanying plot of the friction compensator output versus the velocity showed in Figure 4-23.

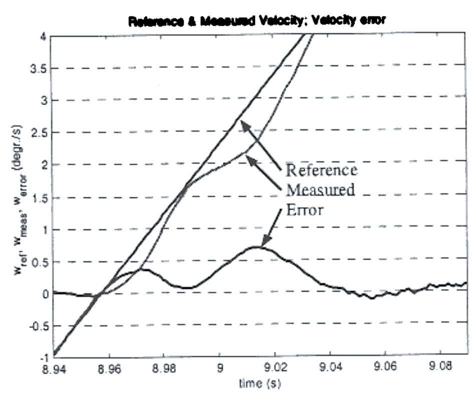

Figure 4-22 Zoom of velocity reversal with limited update LuGre (1) friction compensation

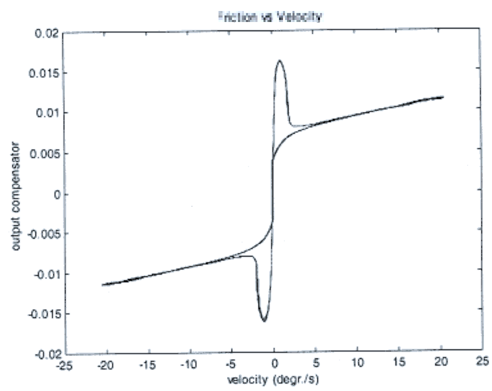

Figure 4-23 Friction compensation versus velocity of limited update adaptive LuGre (1) friction compensation

The velocity error around zero velocity is slightly reduced compared to the 'normal' compensator. The reversal bump however is hardly felt, in spite of the relatively large error. The reason for this is that the course of the measured velocity is smooth; the system never gets stuck and the acceleration is not much higher than the desired acceleration (at least the difference is not perceptible by most humans).

The LuGre friction model of the experiments (Figure 4-23) does not match the LuGre friction model of the simulations (Figure 2-7). Therefore, the results of this experiment are not normative for this compensator. So whether this compensator is capable of reducing the reversal bump significantly is not clear from this experiment. However, due to lack of time a better integration method suitable for this system setup has not been implemented. The integration method should be able to compute the LuGre model for the (relatively small) parameters of table 3-1. There are three possible solutions for this problem. First to increase the sampling rate. The system is now running at a rate of 1000 Hz. The implemented integration method should be able to compute the LuGre model at a higher sampling rate. A second solution could be to implement an integration method that is capable of computing the LuGre model with a frequency of 1000 Hz. The last solution could be an integration method that artifically decrease the stepsize of the integration method for the LuGre model (the system will still be running at 1000 Hz.). When an integration method is found which is capable of computing the LuGre model (so that the obtained LuGre model resembles Figure 2-7) the compensator should be able to better reduce the reversal bump compared to the adaptive LuGre (1) friction compensator which is now implemented. The new compensator should be able to do so without any limited update regime, because the extra bump on the measured velocity (see Figure 4-20) is mainly caused by the large bump on the friction curve, see Figure 4-24. From this figure can be seen that the overshoot bump is caused by the bump on the friction curve.

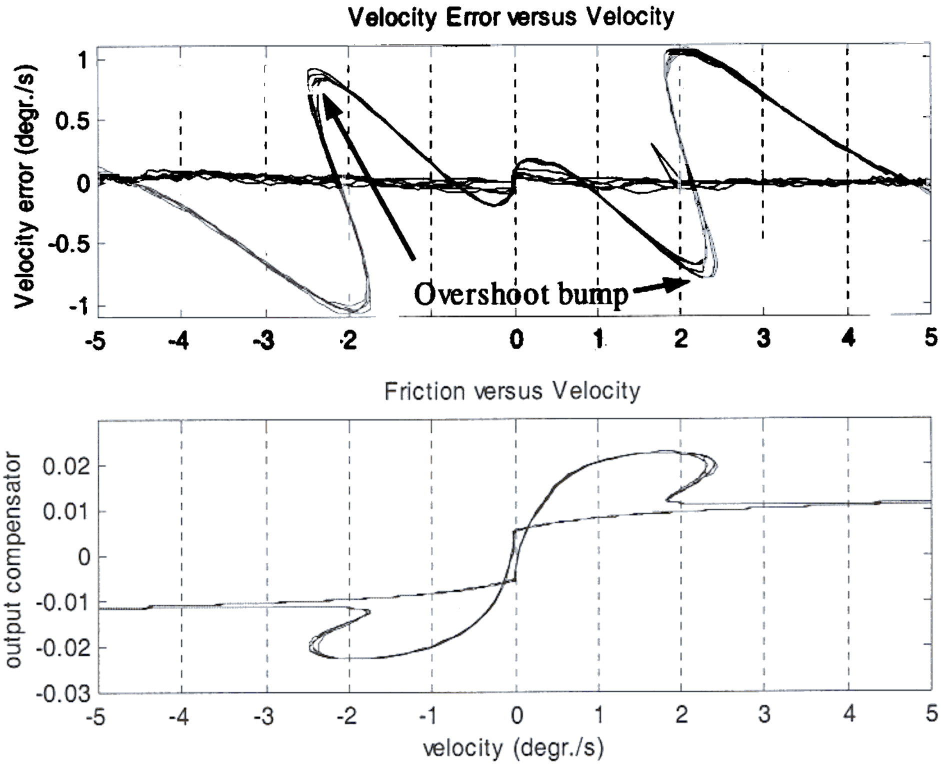

Figure 4-24 Velocity error and Friction compensation versus the velocity for the LuGre (1) compensator without limited update

4.6 System with adaptive LuGre (4) compensation

The compensator design of paragraph 3.4 has been implemented and tested. Although this compensator looks promissing in the literature (Panteley, E. et al., 1998) and during simulations, the friction compensator did not work properly. In Figure 4-25 the velocity reversal of the system with the LuGre (4) friction compensator is depicted.

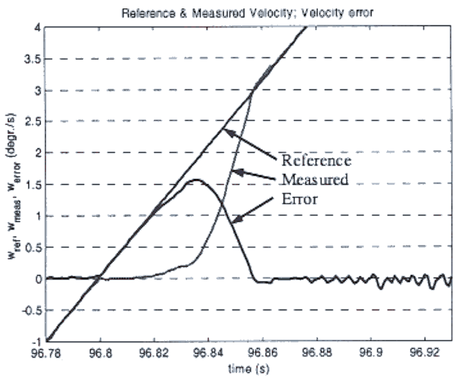

Figure 4-25 Zoom of velocity reversal with the LuGre (4) friction compensator

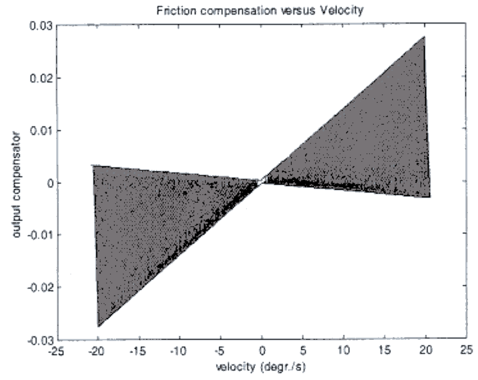

Figure 4-26 Friction compensation versus velocity of the LuGre (4) friction compensation

From Figure 4-25 can be seen that the reversal bump is not reduced at all. The velocity error is still present and as large as without friction compensation. The reason for this malfunctioning is shown in Figure 4-26. In this figure the friction compensation versus the velocity is depicted. The compensator does not compensate for the static friction. In Figure 4-27 the transient behavior of the compensator is depicted.

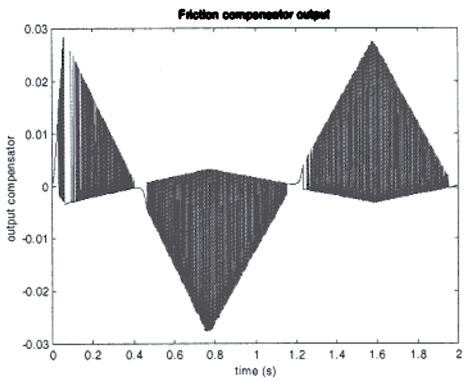

Figure 4-27 The output of the LuGre (4) friction compensator

The output of the compensator is rapidly switching between a positive and a negative value. This is caused by the relay-based compensator (for the friction disturbance part) and the fact that the velocity error is a high frequent fluctuating signal (round zero). Whereas in literature (Canudas de Wit, C. and Lischinsky, P., 1997) the velocity error is a smooth signal.

Another problem is the fact that the parameters do not converge. After a while the parameters become too large and the compensation signal is hearable from the stick. The evolution of the four parameters is shown in Figure 4-28.

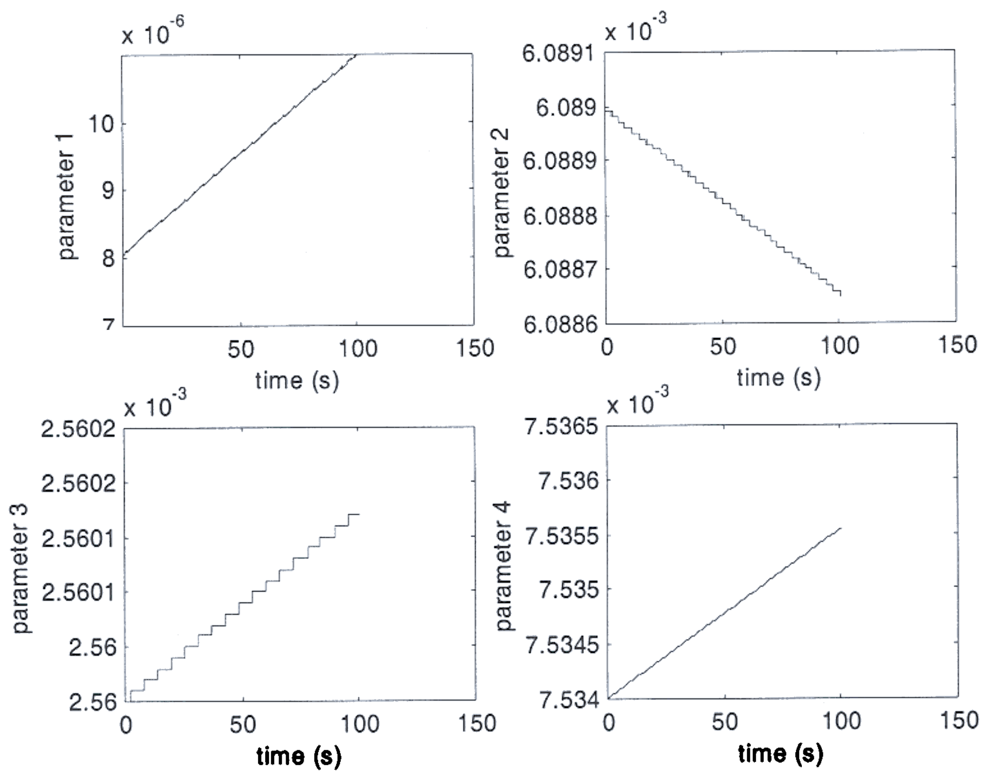

Figure 4-28 Evolution of the four parameters of the LuGre (4) compensator

4.7 Overview of the results

In this section the different friction compensators will be compared with each other. The adaptive LuGre (4) friction compensator does not function properly, therefore this compensator will not be taken into account. So this paragraph will be dealing with the two learning friction compensators (standard LFFFC and the two-distribution LFFFC) and the two adaptive friction compensators (Coulomb friction and LuGre (1) friction).

First there is something remarkable about the two-distribution LFFFC. In (Spreeuwers, L., 1999) this compensator reaches a reduction of a factor 10, whereas the compensator now only reach a reduction of a factor 3. The only difference between the experiments is that the reference signal was slightly different. The turn margin is half the original value for the experiments performed for this thesis (see appendix of (Spreeuwers, L., 1999) and appendix B), but the reference velocity is the same so the system has to reach this velocity sooner, which leads to higher acceleration. Apart from that the setup is the same for both experiments. Even when the experiments were exactly the same the two-distribution LFFFC did not reach a factor 4 reduction. Maybe something is corrupted in the weights file of the LFFFC, so the adaptive friction compensators will compared mainly to the standard LFFFC. This compensator almost reaches the performance of the standard LFFFC of (Spreeuwers, L., 1999), i.e. this compensator reduces the reversal bump by a factor 9 instead of 10.

From the adaptive compensators the simplest is the 'best'. The (adjusted) adaptive Coulomb friction compensator is able to reduce the reversal bump by a factor 7. This is enough to reduce the reversal bump below the level of (human) perception. The adaptive LuGre (1) compensator is also able to reduce the reversal bump, however this is only by a factor 3. The reason for this is that the LuGre model is not computed properly in the compensator. Provided that the integration method for the LuGre model is enhanced, so this model resembles Figure 2-7, this compensator should be capable of reducing the reversal bump even more. The effect of the dynamic friction phenomena on the performance of the FCLS is nil, so the LuGre model gives a surplus of information which has no effect on the performance of the FCLS. The dominant friction phenomena are the static friction phenomena.

Adaptive friction compensation is easy to implement (on already existing controllers). The adaptive Coulomb friction compensation adds at most ten program lines to the software (when implemented directly into the controller(object)). In the case of the adaptive LuGre (1) friction compensator some more program lines are added, depending on the integration method. However, programming the LuGre (1) compensator requires less code than the implementation of the learning friction compensators. In addition the learning friction compensator requires much more memory space to retain the weights of the network. This is usually not a problem, especially in the case of a PC, but when the compensator is implemented on specific embedded hardware, this could give rise to problems. So on the implementation part the adaptive friction compensators (the Coulomb and LuGre (1) friction compensators) are easier to implement on systems than learning friction compensators. And the performance of the Coulomb friction compensator (and probably a good working LuGre (1) friction compensator) is not inferior to the performance of the learning compensators.

The only drawback of the LuGre (1) compensator is the need for proper identification of the model parameters. This drawback does not apply to the Coulomb friction compensator, this compensator is able to estimate the Coulomb friction level from zero. When the friction is the main and dominant phenomenon in a system, the friction can be learned well with a learning friction compensator, and no a-priori knowledge is required. However when other phenomena deteriorate the performance of the system are also present (and not negligible), such as torque ripple of the motor and gravity, the training of the (learning) network can give difficulties (Spreeuwers, L., 1999). When these phenomena are present in a system precautionary measures should be taken, i.e. these phenomena should be compensated for before the learning friction compensator is trained. On the adaptive friction compensators these phenomena have less influence, because the effects of these phenomena are averaged out.

Conclusions and Recommendations

Conclusions on adaptive friction compensation will be drawn in paragraph 5.1. In paragraph 5.2 recommendations for future work on adaptive friction compensation will be given.

5.1 Conclusions

In general the following conclusions can be drawn:

- A proper working friction compensator has been presented that is capable of reducing the reversal bump significantly both in simulations and experiments. This compensator uses the simplest representation of friction (Coulomb friction model) and estimates the Coulomb friction level by means of a non-linear observer. The discontinuous *sign* function of the Coulomb friction model has been substituted by a continuous *tanh* function to smoothen the function.
- A compensator with a more detailed representation of friction (LuGre model) has been designed and implemented. Although this compensator is able to reduce the reversal bump, the compensator does not work properly, because the LuGre model is not computed correctly.
- A LuGre based friction compensator has been presented, that adapts for four parameters. This compensator is able to reduce the effects of friction in simulations, however, in the experiments this compensator was not able to reduce the effects of friction, especially the reversal bump.
- The best adaptive compensator (adaptive Coulomb friction compensator) is not inferior to the learning friction compensators, and this adaptive compensator is easier to implement on a control system.

In regard to the identification of the LuGre friction parameters on the FCLS the following conclusions can be drawn.

- The static parameters of the LuGre model could be identified relatively easy, although the static friction can be estimated more precisely when an encoder was used with higher resolution.
- It was not possible to identify the dynamic parameters of the LuGre model in the present configuration of the system. A position sensor with a higher resolution should be installed in the system when the dynamic parameters should be identified.
- The dominant friction phenomena on the FCLS are the static phenomena.
- The identified values of the parameters seem realistic, i.e., the LuGre model response looks reliable in simulations and in the case of the adaptive Coulomb friction compensator the simulation results correspond to a large extent to the experiments. The model (and its parameters) could not be verified through experiments, because the LuGre model could not be computed correctly in the compensator.

The friction on the FCLS is not direction independent. When a symmetrical reference is applied to the system in open loop, the system has a tendency to one side.

The following conclusions can be drawn when the simulations are regarded:

- The LuGre model is well suited for simulations, it incorporates the most common friction phenomena in a dynamic model, so no additional measures need to be taken like zero velocity detection. The simulations of the Coulomb friction compensator resemble the results of the experiments, which demonstrate the validity of the model. The only drawback of this model is the need of an identification of the model parameters.
- From the simulations it became clear that the original Coulomb friction compensator was overcompensating during a velocity reversal. To overcome this problem two adjustments have been suggested and implemented on the compensator. These adjustments, a smooth function for the transition through zero and only update the parameter in a region around zero velocity, increase the performance of the compensator; a reduction of the reversal bump by a factor 6 was achieved.
- The adaptive LuGre (4) friction compensator performs well in the simulations. It is able to reduce the reversal bump totally.

The next conclusions can be drawn from the experiments performed on the control loading system available at the Control Laboratory:

- Both the compensators that only adapt one parameter are able to reduce the reversal bump. Although the adaptive Coulomb friction compensator uses the simplest friction model, it achieved the best performance of all adaptive compensators. A reduction of the reversal bump of a factor 7 was achieved, this is less than the best learning friction compensator (factor 9), but the reversal bump was not perceptible anymore in the simulation mode of the FCLS. The adaptive LuGre (1) friction compensator achieved also a reduction of the reversal bump, but due to poor computation of the LuGre model in the compensator the level of reduction was disappointing.
- The LuGre (4) friction compensator was not able to reduce the reversal bump at all. This is due to the fact that the velocity error signal is fluctuating heavily, which make the relay based compensation part switching constantly. As a result the parameters do not converge to a proper value.

Finally some conclusions can be drawn when the adaptive friction compensators are compared with learning friction compensation. When the adaptive friction compensators are compared to the learning friction compensators one could say that:

- Adaptive friction compensators are able to reduce the reversal bump, but in general require more a-priori knowledge, there is often the necessity of identification of the parameters, are easy (often easier) to implement and require less memory and are less sensitive to other phenomena on the system like torque ripple.
- Learning friction compensators are able to reduce the reversal bump, for that they require none (or less) a-priori knowledge, they need no identification of parameters, are more difficult to implement and require some memory and are more sensitive to other phenomena on the system.

5.2 Recommendations

In regard to the presented adaptive compensators some recommendations can be made:

- Investigate how the identification of the LuGre model parameters can be enhanced, especially the identification of the dynamic parameters of the model.
- For the FCLS an optimal PI controller could be designed. With such controller the actual performance of the friction compensators on a 'real' system (in normal operation mode) could be verified.
- Investigate how the adaptive Coulomb friction compensator performs on other systems, whether the adjustments made for the FCLS are necessary for other systems.
- Investigate how other static friction models incorporating several of the four static friction phenomena, like the locally developed friction model, perform on the FCLS and whether they are able of giving a further reduction of the reversal bump in regard to the Coulomb friction model.
- The computation of the LuGre model in the LuGre (1) friction compensator should be modified so that the model corresponds to real behavior of the LuGre model (as was found in simulations).
- A profound research could be made to investigate why the LuGre (4) friction compensator has such bad performance and how to improve this compensator.

References

[1] Altpeter, F., Myszkorowski, P., Kocher, M., Longchamp, R., *Friction Compensation: PID Synthesis And State Control*, European Control Conference session TH-M I1, Brussel, 1997

[2] Altpeter, F., Necsulescu, D., Longchamp, R., *Friction Modelling And Identification Issues For Electric Drives*, Electromotion '97, Cluj-Napoca, Romania, May 1997, pp. 149-154

[3] Amin, J., Friedland, B., Harnoy, A., *Implementation of a Friction Estimation and Compensation Technique*, IEEE Control Systems, August 1997, pp. 71-76

[4] Armstrong-Hélouvry, B., *Control of Machines with Friction*, Kluwer Academic Publishers, Boston, ISBN 0-7923-9133-0, 1991

[5] Armstrong-Hélouvry, B., Dupont, P., Wit, C.C. de, *A Survey of Models, Analysis Tools and Compensation Methods for the Control of Machines with Friction*, Automatica, Vol. 30, No. 7, 1994, pp. 1083-1138

[6] Bai, E.W., *Parametrization and Adaptive Compensation of Friction Forces*, International Journal of Adaptive Control and Signal Processing, Vol. 11, 1997, pp. 21-31

[7] Bouwhuis, B.R., *Learning Control of a Flight Simulator Stick*, M. Sc. Thesis, reportnr. 007R99, Control Laboratory, Department of Electrical Engineering, University of Twente, Enschede, The Netherlands, 1999

[8] Breedveld, P.C., *An alternative Model for Static and Dynamic Friction in Dynamic System Simulation,* preliminary report, Cornelis J. Drebbel Institute of Systems Engineering, University of Twente, The Netherlands, 2000

[9] Breemen, A.J.N., *Agent-Based Control Systems Design,* Control Laboratory, Faculty of Electrical Engineering, University of Twente, The Netherlands, 1999

[10] Canudas de Wit, C., Aström, K.J., Braun, K., *Adaptive Friction Compensation in DC-Motor Drives*, IEEE Journal Of Robotics And Automation, Vol. RA-3, No. 6, December 1987, pp. 681-685

[11] Canudas de Wit, C., Lischinsky, P., *Adaptive Compensation with Partially Known Dynamic Friction Model*, International Journal of Adaptive Control and Signal Processing, Vol. 11, 1997, pp. 65-80

[12] Canudas de Wit, C., Olssen, H., Aström K.J., Lischinsky, P., *A New Model for Control of Systems with Friction*, IEEE Transactions On Automatic Control, Vol. 40, No. 3, March 1995, pp. 419-425

13] C. Canudas de Wit (In collabortion with: K.J. Astrom, and M. Sorin), "*Slides of the Workshop on Control of systems with friction*", Material of the Workshop presented at: the IEEE Conference on Decision and Control CDC'98, Dec. Florida, USA, and at the IEEE Conference on Control Applications CCA'99, August 22-27, Hawaii, USA.

[14] Feemster, M., Vedagarbha, P., Dawson, D.M., Haste, D., *Adaptive control techniques for friction compensation*, Mechatronics, 9, 1999, pp. 125-145

15] Friedland, B., Park, Y.J., *On Adaptive Friction Compensation*, IEEE Transactions on Automatic Control, Vol. 37, No. 10, October 1992, pp. 1609-1612

[16] Gäfvert, M., *Comparison of Two Dynamic Friction Models*, M.Sc. Thesis, reportnr. ISRN LUTFD2/TFRT–5561–SE, Department of Automatic Control, Lund Institute of technology, Lund, Sweden, June 1996

[17] Leonard, N.E., Krishnaprasad, P.S., *Adaptive Friction Compensation for Bi-Directional Low-Velocity Position Tracking*, Technical Research Report, reportnr. TR 92-91, Electrical Engineering Department & Systems Research Center, University of Maryland, 1992

18] Lischinsky, P., Wit, C.C. de, Morel, G., *Friction Compensation for an Industrial Hydraulic Robot*, IEEE Control Systems, February 1999, pp. 25-32

[19] Olsson, H., Aström, K.J., Canudas de Wit, C., Gäfvert, M., Lischinsky, P., *Friction models and friction compensation*, European Journal of Control, Vol. 4, 1998, pp. 176-195

[20] Panteley, E., Ortega, R., Gäfvert, M., *An Adaptive Friction Compensator for Global Tracking in Robot Manipulators*, Systems & control letters, ISSN 0167-6911, Vol. 33, nr. 5, 1998, pp. 307-313

[21] Slotine, J.J.E., Li, W., *On the adaptive control of robot manipulators*, The International Journal of Robotics Research, Vol. 6, No. 3, 1987, pp. 49-59

[22] Spreeuwers, L., *Learning Friction Compensation*, M. Sc. Thesis, reportnr. 040R99, Control Laboratory, Department of Electrical Engineering, University of Twente, Enschede, The Netherlands, 1999

Appendix A

Description of simulation with control loading system without friction compensation

20-sim Experiment Description
==============================

Model:	model
Experiment:	Fokker_Stick1 static

Parameters:
===========

PI_controller\kp	0.005
PI_controller\tauI	0.01
WaveGenerator1\amplitude	20
WaveGenerator1\omega	1
Motor_contant\K	0.16
I1\i	7.8911e-006
Lugrefriction \F_coulomb	0.0020388
Lugrefriction \F_static	0.00256
Lugrefriction \F_viscous	8.9044e-005
Lugrefriction \v_stribeck	0.0095633
Lugrefriction \sigma_1	0.06
Lugrefriction \sigma_0	100
Coulomb_Fric_Comp2\k	0
Coulomb_Fric_Comp2\mu	0
Coulomb_Fric_Comp2\lambda	0
Coulomb_Fric_Comp2\vmargin	

Initial Values:
===============

PI_controller\state_initial	0
I1\state_initial	0
Submodel2\z_init	0
Coulomb_Fric_Comp2\z_init	0

Run Specifications:
===================

StartTime:	0
FinishTime:	20
Output After Each:	1e-005
Integration Method:	MeBDFiMethod

Absolute Tolerance:	1e-008
Relative Tolerance:	1e-008
Algebraic Loop Absolute Tolerance:	1e-008
Algebraic Loop Relative Tolerance:	1e-008
Use Fixed Step Size:	FALSE

Description of simulation with control loading system with adaptive Coulomb friction compensation

20-sim Experiment Description

==========================

Model:	model
Experiment:	Fokker_Stick1 static

Parameters:

==========

PI_controller\kp	0.005
PI_controller\tauI	0.01
WaveGenerator1\amplitude	20
WaveGenerator1\omega	
Motor_contant\K	0.16
I1\i	7.8911e-006
Lugrefriction \F_coulomb	0.0020388
Lugrefriction \F_static	0.00256
Lugrefriction \F_viscous	8.9044e-005
Lugrefriction \v_stribeck	0.0095633
Lugrefriction \sigma_1	0.06
Lugrefriction \sigma_0	100
Coulomb_Fric_Comp2\k	1e-006
Coulomb_Fric_Comp2\mu	0.5
Coulomb_Fric_Comp2\lambda	100
Coulomb_Fric_Comp2\vmargin	4

Initial Values:

=============

PI_controller\state_initial	0
I1\state_initial	0
Submodel2\z_init	0
Coulomb_Fric_Comp2\z_init	0.014

Run Specifications:

==================

StartTime:	0
FinishTime:	20
Output After Each:	1e-005
Integration Method:	MeBDFiMethod
Absolute Tolerance:	1e-008
Relative Tolerance:	1e-008

Algebraic Loop Absolute Tolerance:	1e-008
Algebraic Loop Relative Tolerance:	1e-008
Use Fixed Step Size:	FALSE

Description of simulation with control loading system with adaptive LuGre (1) friction compensation

20-sim Experiment Description
============================

Model:	model
Experiment:	Fokker_Stick1 lugre

Parameters:
===========

PI_controller\kp	0.005
PI_controller\tauI	0.01
WaveGenerator1\amplitude	20
WaveGenerator1\omega	
Motor_contant\K	0.16
I1\i	7.8911e-006
Lugrefriction\F_coulomb	0.0020388
Lugrefriction \F_static	0.00256
Lugrefriction \F_viscous	8.9044e-005
Lugrefriction \v_stribeck	0.0095633
Lugrefriction \sigma_1	0.06
Lugrefriction \sigma_0	100
Lugre1_Fric_Comp2\k	1e-006
Lugre1_Fric_Comp2\mu	0.5
Lugre1_Fric_Comp2\lambda	
Lugre1_Fric_Comp2\vmargin	4
Lugre1_Fric_Comp2\F_coulomb	0.0020388
Lugre1_Fric_Comp2\F_static	0.00256
Lugre1_Fric_Comp2\F_viscous	8.9044e-005
Lugre1_Fric_Comp2\v_stribeck	0.0095633
Lugre1_Fric_Comp2\sigma_0	100
Lugre1_Fric_Comp2\sigma_1	0.06

Initial Values:
===============

PI_controller\state_initial	0
I1\state_initial	
Submodel2\z_init	0
Lugre1_Fric_Comp2\z_init	6.25
Lugre1_Fric_Comp2\s_init	0

Run Specifications:
===================

StartTime:	0
FinishTime:	10
Integration Method:	MeBDFiMethod

Absolute Tolerance:	1e-008
Relative Tolerance:	1e-008
Algebraic Loop Absolute Tolerance:	1e-008
Algebraic Loop Relative Tolerance:	1e-008
Use Fixed Step Size:	FALSE

Description of simulation with control loading system with adaptive LuGre (4) friction compensation

20-sim Experiment Description
===========================

Model:	model
Experiment:	Fokker_Stick lugre4

Parameters:
==========

mass\i	0.00024			
PI_controller\kp	0.15			
PI_controller\tauI	0.005			
R_LuGre\F_coulomb	0.1132			
R_LuGre\F_static	0.175			
R_LuGre\F_viscous	0.0026			
R_LuGre\v_stribeck	0.01			
R_LuGre\sigma_1	0.309839			
R_LuGre\sigma_0	100			
WaveGenerator1\amplitude	20			
WaveGenerator1\omega	1			
Motor_contant\K	1			
LuGreComp\gamma	[1,	0,	0,	0;
	0,	1,	0,	0;
	0,	0,	1,	0;
	0,	0,	0,	
LuGreComp\mu	1000			
LuGreComp\lambda	1			
LuGreComp\theta1_init	0			
LuGreComp\theta2_init	0			
LuGreComp\theta3_init	0			
LuGreComp\theta4_init	0			

Initial Values:
=============

mass\state_initial	0
PI_controller\state_initial	0
R_LuGre\z_init	0
LuGreComp\x_d_initial	0
LuGreComp\x_initial	0

Run Specifications:
=================

StartTime:	0

FinishTime:	10
Integration Method:	MeBDFiMethod
Absolute Tolerance:	1e-008
Relative Tolerance:	1e-008
Algebraic Loop Absolute Tolerance:	1e-008
Algebraic Loop Relative Tolerance:	1e-008
Use Fixed Step Size:	FALSE

Appendix B

Description of experiment with control loading system without compensation

Experimental setup file
=====================

file name: d:/fcls/fclscode/orig.exp

Experiment
----
generator:
Constant Velocity
sensor:
ELC Sensor
controller:
Original Controller
actuator:
ELC Actuator
storer:
Storer
view:
View
timer:
Timer
delayed actuation:
FALSE

Constant Velocity
----
vref: velocity:
20
xa: travel pos:
0.1
xb: turn margin:
8

ELC Sensor

Force Gain:
200
Force Offset:
-0.243
Position Gain:
0.000757545
Position Offset:
22610
Tacho Gain:
-4.226288
Tacho Offset:
-0.0022
Encoder Initialize:
1
Tacho Filter:
SomeFile.mat

Original Controller

Position limit:
15
Velocity limit:
60
K:
0.005
tau_I:
0.01
b:
1
anti windup:
0.03
tame_I:
1
Ka:
0
Kp:
0

ELC Actuator

Inhibit:
FALSE
minimum:
-4.8
maximum:
4.8

Storer
------
store elements:
TRUE
cyclic buffer:
TRUE
number elements:
10000

Timer
-----
frequency:
1000

View

Active:
TRUE
title:
force, reference acceleration
show grid:
TRUE
auto rescale:
TRUE
auto refresh:
TRUE
x-axis title:
time (s)
x-axis minimum:
0
x-axis maximum:
5
y-axis title:
f, a_ref
y-axis minimum:
-100
y-axis maximum:
100

View

Active:
TRUE
title:
reference and measured velocity
show grid:
TRUE
auto rescale:
TRUE
auto refresh:
TRUE
x-axis title:
time (s)
x-axis minimum:
0
x-axis maximum:
5
y-axis title:
w_ref, w_meas, w_error
y-axis minimum:
-60
y-axis maximum:
60

View

Active:
TRUE
title:
reference and measured position
show grid:
TRUE
auto rescale:
TRUE
auto refresh:
TRUE
x-axis title:
time (s)
x-axis minimum:
0
x-axis maximum:
5
y-axis title:
p_ref, p_meas, p_meas_stick

y-axis minimum:
-15
y-axis maximum:
15

View

Active:
TRUE
title:
Control values
show grid:
TRUE
auto rescale:
TRUE
auto refresh:
TRUE
x-axis title:
time (s)
x-axis minimum:
0
x-axis maximum:
5
y-axis title:
P, I, PIout, total control
y-axis minimum:
-0.05
y-axis maximum:
0.05

Description of experiment with control loading system with standard LFFFC

Experimental setup file
======================

file name: d:/fcls/fclscode/slfffc.exp
time/date: Wed Oct 13 19:11:24 1999

Experiment
----
generator:
Constant Velocity
sensor:
ELC Sensor
controller:
Standard LFFFC Controller
actuator:
ELC Actuator
storer:
Storer
view:
View
timer:
Timer
delayed actuation:
FALSE

Constant Velocity
----
vref: velocity:
20
xa: travel pos:
0.1
xb: turn margin:
8

ELC Sensor

Force Gain:
200
Force Offset:
-0.243
Position Gain:
0.000757545
Position Offset:
22610
Tacho Gain:
-4.226288
Tacho Offset:
-0.0022
Encoder Initialize:
1
Tacho Filter:
SomeFile.mat

Standard LFFFC Controller
------ --------
Position limit:
15
Velocity limit:
60
K:
0.005
tau_I:
0.01
b:
1
anti windup:
0.03
tame_I:
1
Ka:
0
Kp:
0
1 distr midzero BSN:
sLFC midzero
nr of splines:
501
learning rate:
0.1
min input:
-30
max input:
30
weights file:
standard.wgt
load weights:
0
save weights:
1
circular:
0
on-(1) or offline(0):
0
normalized:
1

ELC Actuator

Inhibit:
FALSE
minimum:
-4.8
maximum:
4.8

Storer
------
store elements:
TRUE
cyclic buffer:
TRUE
number elements:
10000

Timer
-----
frequency:
1000

View

Active:
TRUE
title:
velocity error
show grid:
TRUE
auto rescale:
TRUE
auto refresh:
TRUE
x-axis title:
time (s)
x-axis minimum:
0
x-axis maximum:
5
y-axis title:
f, a_ref
y-axis minimum:
-100
y-axis maximum:
100

View

Active:
TRUE
title:
reference and measured velocity
show grid:
TRUE
auto rescale:
TRUE
auto refresh:
TRUE
x-axis title:
time (s)
x-axis minimum:
0
x-axis maximum:
5
y-axis title:
w_ref, w_meas, w_error
y-axis minimum:
-50
y-axis maximum:
50

View

Active:
TRUE
title:
reference and measured position

show grid:
TRUE
auto rescale:
TRUE
auto refresh:
TRUE
x-axis title:
time (s)
x-axis minimum:
0
x-axis maximum:
5
y-axis title:
p_ref, p_meas, p_meas_stick
y-axis minimum:
-15
y-axis maximum:
15

View

Active:
TRUE
title:
Control values
show grid:
TRUE
auto rescale:
TRUE
auto refresh:
TRUE
x-axis title:
time (s)
x-axis minimum:
0
x-axis maximum:
5
y-axis title:
P, I, PIout, total control
y-axis minimum:
-0.05
y-axis maximum: 0.05

Description of experiment with control loading system with two distribution LFFFC

Experimental setup file
=======================

file name: d:/fcls/fclscode/2dlfffc.exp
time/date: Thu Oct 14 14:54:47 1999

Experiment
----
generator:
Constant Velocity
sensor:
ELC Sensor
controller:
Two Distribution LFFFC Controller
actuator:
ELC Actuator
storer:
Storer
view:
View
timer:
Timer
delayed actuation:
FALSE

Constant Velocity
----
vref: velocity:
20
xa: travel pos:
0.1
xb: turn margin:
8

ELC Sensor

Force Gain:
200
Force Offset:
-0.243
Position Gain:
0.000757545
Position Offset:
22610
Tacho Gain:
-4.226288
Tacho Offset:
-0.0022
Encoder Initialize:
1
Tacho Filter:
SomeFile.mat

Two Distribution LFFFC Controller

Position limit:
15
Velocity limit:
60
K:
0.005
tau_I:
0.01
b:
1
anti windup:
0.05
tame_I:
1
Ka:
0
Kp:
0
2 distr BSN midzero:
2 distr LFC midzero
nr of splines midregion:
51
nr of splines sideregion:
10
learning rate:
0.08
min input:
-30
min input midregion:
-2.5
max input midregion:
2.5
max input:
30
weights file:
2distr.wgt
load weights:
0
save weights:
1
circular:
0
on-(1) or offline(0):
0
normalized:
1

ELC Actuator

Inhibit:
FALSE
minimum:
-4.8
maximum:
4.8

Storer
------
store elements:
FALSE
cyclic buffer:
FALSE
number elements:
5000

Timer

frequency:
1000

View

Active:
TRUE
title:
velocity error
show grid:
TRUE
auto rescale:
TRUE
auto refresh:
TRUE
x-axis title:
time (s)
x-axis minimum:
0
x-axis maximum:
5
y-axis title:
f, a_ref, w_error
y-axis minimum:
-100
y-axis maximum:
100

View

Active:
TRUE
title:
reference and measured velocity
show grid:
TRUE
auto rescale:

TRUE
auto refresh:
TRUE
x-axis title:
time (s)
x-axis minimum:
0
x-axis maximum:
5
y-axis title:
w_ref, w_meas, w_error
y-axis minimum:
-50
y-axis maximum:
50

View

Active:
TRUE
title:
reference and measured position
show grid:
TRUE
auto rescale:
TRUE
auto refresh:
TRUE
x-axis title:
time (s)
x-axis minimum:
0
x-axis maximum:
5
y-axis title:
p_ref, p_meas, p_meas_stick
y-axis minimum:
-15
y-axis maximum:
15

View

Active:
TRUE
title:
Control values
show grid:
TRUE
auto rescale:
TRUE
auto refresh:
TRUE
x-axis title:
time (s)
x-axis minimum:
0
x-axis maximum:
5
y-axis title:
P, I, PIout, total control
y-axis minimum:
-0.05
y-axis maximum:
0.05

Description of experiment with control loading system with adaptive Coulomb friction compensation

Experimental setup file
======================

file name:
d:/fclsadap/fclacode/coulomb.exp
time/date: Wed Jun 6 02:04:18
2001

Experiment
----
generator:
Constant Velocity
sensor:
ELC Sensor
controller:
Limited Update 2 Adaptive
Coulomb FC Controller
actuator:
ELC Actuator
storer:
ELCStorer
view:
View
timer:
Timer
delayed actuation:
FALSE

Constant Velocity
----
vref: velocity:
20
xa: travel pos:
0.1
xb: turn margin:
4

ELC Sensor

Force Gain:
200
Force Offset:
-0.243
Position Gain:
0.000757545
Position Offset:
22610
Tacho Gain:
-4.226288
Tacho Offset:
-0.0022
Encoder Initialize:
1
Tacho Filter:
SomeFile.mat

Limited Update 2 Adaptive
Coulomb FC Controller

Position limit:
15
Velocity limit:
60
K:
0.005
tau_I:
0.01
b:
1
anti windup:
0.05
tame_I:
1
Ka:
0
Kp:
0
Mu:
0.5
K:
1e-06
factor:

z_init:
0.011
mu of tanh:
4
FeedBack ?:
0
Update Velocity Margin:
4

ELC Actuator

Inhibit:
FALSE
minimum:
-4.8
maximum:
4.8

ELCStorer
----
store elements:
TRUE
cyclic buffer:
FALSE
skip sample elements:
FALSE
number elements:
100000
number of elements to skip:
99

Timer
-----
frequency:
1000

View

Active:
TRUE
title:
Current View
show grid:
FALSE
auto rescale:
TRUE
auto refresh:
TRUE
x-axis title:
time
x-axis minimum:
0

x-axis maximum:
10
y-axis title:
Force, error
y-axis minimum:
-5
y-axis maximum:
5

View

Active:
TRUE
title:
Velocity View
show grid:
FALSE
auto rescale:
TRUE
auto refresh:
TRUE
x-axis title:
time
x-axis minimum:
0
x-axis maximum:
10
y-axis title:
wm,wr,w_error
y-axis minimum:
-50
y-axis maximum:
50

View

Active:
TRUE
title:
Position View
show grid:
FALSE
auto rescale:
TRUE
auto refresh:
TRUE
x-axis title:
time
x-axis minimum:
0
x-axis maximum:
10
y-axis title:
ps, pm, pr
y-axis minimum:
-10
y-axis maximum:
10

View

Active:
TRUE
title:
Control View
show grid:
FALSE
auto rescale:
TRUE
auto refresh:
TRUE
x-axis title:
time
x-axis minimum:
0
x-axis maximum:
10
y-axis title:
PI, FricComp
y-axis minimum:
-0.1
y-axis maximum:
0.1

Description of experiment with control loading system with adaptive LuGre (1) friction compensation

Experimental setup file
========================

file name:
d:/fclsadap/fclacode/lugre1p.exp
time/date: Wed Jun 6 02:14:09
2001

Experiment
----
generator:
Constant Velocity
sensor:
ELC Sensor
controller:
Adaptive One Parameter LuGre
FC Controller
actuator:
ELC Actuator
storer:
ELCStorer
view:
View
timer:
Timer
delayed actuation:
FALSE

Constant Velocity
----
vref: velocity:
20
xa: travel pos:
0.1
xb: turn margin:
4

ELC Sensor

Force Gain:
200
Force Offset:
-0.243
Position Gain:
0.000757545
Position Offset:
22610
Tacho Gain:
-4.226288
Tacho Offset:
-0.0022
Encoder Initialize:
1
Tacho Filter:
SomeFile.mat

Adaptive One Parameter LuGre
FC Controller

-
Position limit:
15
Velocity limit:
60
K:
0.005
tau_I:
0.01
b:
1
anti windup:
0.05
tame_I:
1
Ka:
0
Kp:
0
Mu:
0.5
K:
1e-06
sigma0:
1
sigma1:
0.006
Stribeck velocity:
0.009563
Fcoulomb:
0.002039
Fviscous:
8.9044e-05
Fstatic:
0.00256
FeedForward?:
1
factor:
1
integration factor:
1
Mu tanh:
1000
theta init:
2.278
tameI int z:
0.99
tauI int z:
20
anti windup int z:
0.01
velocity margin:
4

ELC Actuator

Inhibit:
FALSE

minimum:
-4.8
maximum:
4.8

ELCStorer

store elements:
TRUE
cyclic buffer:
FALSE
skip sample elements:
FALSE
number elements:
10000
number of elements to skip:
100

Timer

frequency:
1000

View

Active:
TRUE
title:
Current View
show grid:
FALSE
auto rescale:
TRUE
auto refresh:
TRUE
x-axis title:
time
x-axis minimum:
0
x-axis maximum:
10
y-axis title:
Force, error
y-axis minimum:
-5
y-axis maximum
5

View

Active:
TRUE
title:
Velocity View
show grid:
FALSE
auto rescale:
TRUE
auto refresh:
TRUE
x-axis title:
time
x-axis minimum:
0
x-axis maximum:
10
y-axis title:
wm,wr,w_error
y-axis minimum:
-50
y-axis maximum:
50

View

Active:
TRUE
title:
Position View
show grid:
FALSE
auto rescale:
TRUE
auto refresh:
TRUE
x-axis title:
time
x-axis minimum:
0
x-axis maximum:
10
y-axis title:
ps, pm, pr
y-axis minimum:
-10
y-axis maximum:
10

View

Active:
TRUE
title:
Control View
show grid:
FALSE
auto rescale:
TRUE
auto refresh:
TRUE
x-axis title:
time
x-axis minimum:
0
x-axis maximum:
10
y-axis title:
PI, FricComp
y-axis minimum:
-0.1
y-axis maximum:
0.1

Description of experiment with control loading system with adaptive LuGre (4) friction compensation

Experimental setup file
========================

file name:
d:/fclsadap/fclacode/lugre4p.exp
time/date: Wed Jun 6 02:17:07
2001

Experiment

generator:
Constant Velocity
sensor:
ELC Sensor
controller:
Adaptive LuGre FC Controller
actuator:
ELC Actuator
storer:
ELCStorer
view:
View
timer:
Timer
delayed actuation:
FALSE

Constant Velocity
----
vref: velocity:
20
xa: travel pos:
0.1
xb: turn margin:
4

ELC Sensor

Force Gain:
200
Force Offset:
-0.243
Position Gain:
0.000757545
Position Offset:
22610
Tacho Gain:
-4.226288
Tacho Offset:
-0.0022
Encoder Initialize:
1
Tacho Filter:
SomeFile.mat

Adaptive LuGre FC Controller

Position limit:
15
Velocity limit:
60
K:
0.005
tau_I:
0.01
b:

anti windup:
0.05
tame_I:
1
Ka:
0
Kp:
0
Mu:
1000
gamma (GAMMA=gamma*I)
0.0001
Lambda:

Theta_init1

7.8911e-06
Theta_init2:
8.9e-05
Theta_init3:
0.00256
Theta_init4:
0.007534
factor :
0.01

ELC Actuator

Inhibit:
FALSE

-4.8
maximum:
4.8

ELCStorer
----
store elements:
TRUE
cyclic buffer:
FALSE
skip sample elements:
TRUE
number elements:
10000
number of elements to skip:
99

Timer
-----
frequency:
1000

View

Active:
TRUE
title:
Current View
show grid:
FALSE
auto rescale:
TRUE
auto refresh:
TRUE
x-axis title:
time
x-axis minimum:
0
x-axis maximum:
10
y-axis title:
Force, error
y-axis minimum:
-5
y-axis maximum:
5

View

Active:
TRUE
title:
Velocity View
show grid:
FALSE
auto rescale:
TRUE
auto refresh:
TRUE
x-axis title:
time
x-axis minimum:
0
x-axis maximum:
10
y-axis title:
wm,wr,w_error
y-axis minimum:
-50
y-axis maximum:
50

View

Active:
TRUE
title:
Position View
show grid:
FALSE
auto rescale:
TRUE
auto refresh:
TRUE
x-axis title:
time
x-axis minimum:
0
x-axis maximum:
10
y-axis title:
ps, pm, pr
y-axis minimum:
-10
y-axis maximum:
10

View

Active:
TRUE
title:
Control View
show grid:
FALSE
auto rescale:
TRUE
auto refresh:
TRUE
x-axis title:
time
x-axis minimum:
0
x-axis maximum:
10
y-axis title:
PI, FricComp
y-axis minimum:
-0.1
y-axis maximum:
0.1